

Probing the Active Site of LpxC in Gram-Negative Bacteria:  
Design and Synthesis of Acyclic Natural Substrate Analogues

Sarah Nicole Malkowski

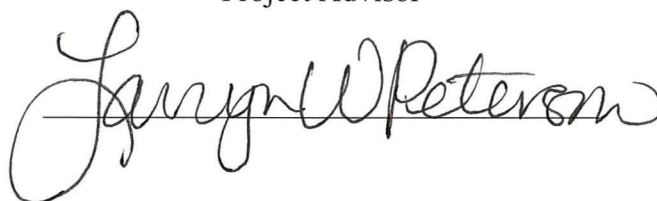
Department of Chemistry  
Rhodes College  
Memphis, Tennessee

2014

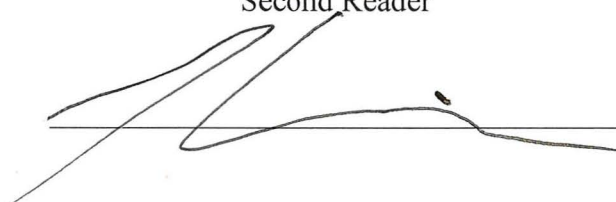
Submitted in partial fulfillment of the requirements for the  
Bachelor of Science degree with Honors in Chemistry

This Honors paper by Sarah Malkowski has been read and approved for Honors in Chemistry.

Dr. Larryn W. Peterson  
Project Advisor

A handwritten signature in cursive script that reads "Larryn W. Peterson". The signature is written in black ink and is positioned above a horizontal line.

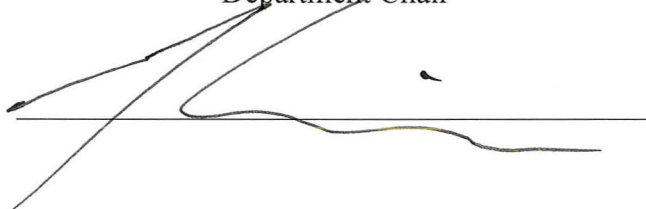
Dr. Mauricio Cafiero  
Second Reader

A handwritten signature in cursive script that reads "Mauricio Cafiero". The signature is written in black ink and is positioned above a horizontal line.

Dr. Laura Luque de Johnson  
Extra-Departmental Reader

A handwritten signature in cursive script that reads "Laura Luque de Johnson". The signature is written in black ink and is positioned above a horizontal line.

Dr. Mauricio Cafiero  
Department Chair

A handwritten signature in cursive script that reads "Mauricio Cafiero". The signature is written in black ink and is positioned above a horizontal line.

## ACKNOWLEDGEMENTS

I would like to thank Dr. Peterson for all of her guidance and support throughout my research experience. Thank you to Christopher Grubb for his work on this project, especially the alkylation work. I would also like to thank the other lab members in our group, Gabrielle Bailey, and Jennifer Rote. Thank you to Dr. Cafiero, Allison Dewar, and A. Katherine Hatstat for their work on the computational studies of LpxC and our analogues. I thank Dr. Kimberly Brien, Dr. Roberto de Salud Bea, as well as the rest of the Chemistry Department. Lastly, I would like to thank my friends and family for all of the support that they have offered me.

## CONTENTS

Signature page	ii
Acknowledgements	iii
Contents	iv
List of Figures	v
List of Tables	vi
List of Schemes	vii
Abstract	viii
Introduction	1
Experimentals	10
Results and Discussion	21
Conclusion	29
References	30
Appendix	35

## LIST OF FIGURES

Figure 1. Depiction of Gram-negative bacterial membrane	1
Figure 2. UDP and palmitate bound in LpxC (PDB 2IER)	2
Figure 3. LpxC with CHIR-090 bound in active site	3
Figure 4. Previously developed inhibitors of LpxC	4
Figure 5. A) The structure of the natural substrate; B) The general structure of proposed analogues	6
Figure 6. UDP-(3-O-(R-3-hydroxymyristoyl))-glucosamine bound in the LpxC active site with residues in polar region and hydrophobic pocket included (PDB 4MDT).	7
Figure 7. UDP bound in LpxC with important residues included (PDB 2IER).	7
Figure 8. A) Triazole-linked analogue; B) Ether-linked analogue	8
Figure 9. Structures of proposed natural substrate analogues	9

## LIST OF TABLES

Table 1. Reagents and results for the formation of the acyclic tosylate	25
Table 2. Reagents and results for the attempted conversion of the carboxylic acid to the hydroxamic acid	28

## LIST OF SCHEMES

Scheme 1. Synthesis of the ribose ether-linked carboxylic acid (SA-001)	22
Scheme 2. Synthesis of the ribose triazole-linked carboxylic acid (SA-004)	23
Scheme 3. Synthesis of the acyclic uracil-based nucleoside	24
Scheme 4. Synthesis of the acyclic triazole-linked carboxylic acid (SA-003)	24
Scheme 5. Synthesis of the acyclic ether-linked carboxylic acid (SA-005)	26
Scheme 6. Synthesis of the ribose triazole-linked analogue (SA-002)	29

## ABSTRACT

Probing the Active Site of LpxC in Gram-Negative Bacteria: Design and Synthesis of  
Acyclic Natural Substrate Analogues

by

Sarah Nicole Malkowski

Currently, there are limited therapies to effectively treat Gram-negative bacterial infections. Compared to Gram-positive bacteria, Gram-negative bacteria have an additional peptidoglycan outer membrane composed of lipopolysaccharide (LPS). Lipid A, an integral component of LPS, is essential for bacterial virulence and pathogenicity. LpxC catalyzes the first committed step in the biosynthetic pathway of lipid A, making it an attractive target for inhibition. This work focuses on probing the active site of LpxC through the synthesis of natural substrate analogues in order to develop a novel broad-spectrum inhibitor. The natural substrate has three key features to bind in the active site: a nucleoside containing uracil to bind in the polar region, a diphosphate to coordinate to the zinc ion, and a substituted glucosamine with a long hydrocarbon chain to interact with the residues in the hydrophobic passage. With this in mind, the analogues contain uracil bound to a ribose or acyclic sugar that is connected to an amino acid-containing hydroxamic acid through an ether linkage or triazole linkage. Four analogues, two with the ribose and two with the acyclic sugar, were synthesized to their carboxylic acid intermediates, and a method has been determined to convert the carboxylic acid intermediate to the hydroxamic acid compound. An analogue containing uridine coupled to an amino acid-containing hydroxamic acid via a triazole linker was successfully synthesized in seven steps.



I give permission for public access to my Honors paper and for any copying or digitization to be done at the discretion of the College Archivist and/or the College Librarian.

Signed 

Sarah Malkowski

Date 05/11/2014

## I. Introduction

### A. Background

Although there have been many great technological advances in the health industry, the treatment of microbial diseases, including bacterial, viral, and parasitic infections, remains a challenge.<sup>1</sup> Many of these infections are now commonly found in hospitals and local clinics and have developed resistance mechanisms to current antibiotic drug treatments.<sup>2,3</sup> It was estimated in 2002 that two million bacterial infections resulted in 99,000 deaths in the United States alone.<sup>4</sup> Among the culprits of such infections are Gram-negative bacteria, such as *E. coli* and *P. aeruginosa*.<sup>2,3,5</sup> To further complicate the issue, multidrug-resistant strains of Gram-negative bacteria present potential serious health issues.<sup>5</sup> In 2008, data demonstrated 13% of *E. coli* and 17% of *P. aeruginosa* were multidrug-resistant.<sup>5</sup> The rise in bacterial resistance and the difficulty in treating Gram-negative bacterial infections have prompted researchers to develop novel effective antibacterial therapies.<sup>2</sup>

Gram-negative bacteria differ from Gram-positive bacteria in the composition of their cell walls. Both Gram-positive and Gram-negative bacteria have a cytoplasmic

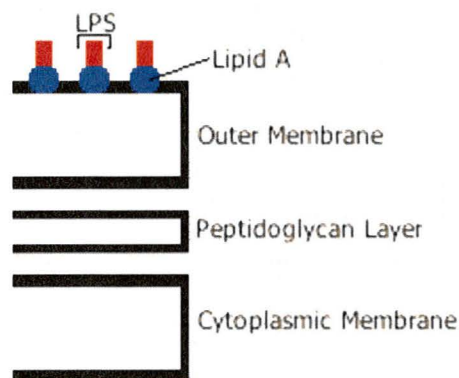


**Figure 1.** Depiction of Gram-negative bacterial membrane

membrane and peptidoglycan layer, but Gram-negative bacteria have an additional outer membrane (Figure 1). The outer membrane serves as a selectively permeable barrier, which decreases the efficacy of many antibiotics.<sup>6</sup>

The outer membrane of Gram-negative bacteria is composed of lipopolysaccharide (LPS).

LPS is also known as endotoxin, and when released from dying bacteria into the body, it can induce septic shock, or septicemia.<sup>5</sup> Septicemia was the tenth leading cause of death in the United States in 2010.<sup>5</sup> An integral component of LPS is Lipid A, which is a glucosamine-based phospholipid. Lipid A anchors LPS to the outer membrane and is essential for the growth and viability of the bacterium.<sup>2</sup> Thus, inhibition of the biosynthesis of Lipid A is an attractive approach for developing new antibacterial therapies.

### *B. LpxC*

There are nine enzymes involved in the biosynthetic pathway of Lipid A.<sup>5</sup> Among these enzymes is LpxC, or UDP-3-O-(*R*-3-hydroxymyristoyl)-*N*-acetylglucosamine deacetylase, which removes an acetyl group from the nitrogen on the substituted glucosamine to form a primary amine. LpxC is responsible for catalyzing the first committed step of the pathway, which means that after this step is completed, there is a full commitment to synthesize lipid A.<sup>5</sup> Hence, LpxC is an attractive target for inhibiting the synthesis of lipid A, as inhibition of LpxC would prevent the synthesis of Lipid A and result in a compromised outer membrane. Several LpxC inhibitors have already been

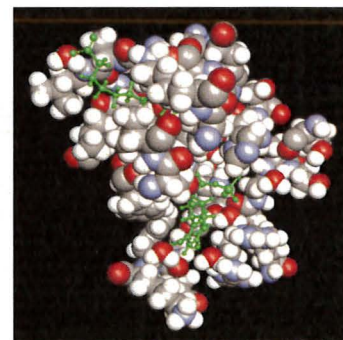


**Figure 2.** UDP and palmitate bound in LpxC (PDB 2IER).<sup>7</sup>

developed, but many of them have a limited range of activity against different strains of Gram-negative bacteria.<sup>6</sup> For example, some compounds have successfully inhibited the growth of *E. coli*, but not *P. aeruginosa*.<sup>6</sup> A consequence of this work has been the determination of the crystal structure of LpxC. The solvation of crystal structures has

provided important information about interactions between critical residues in LpxC and bound ligands. From the crystal structure, three features have been identified in the LpxC

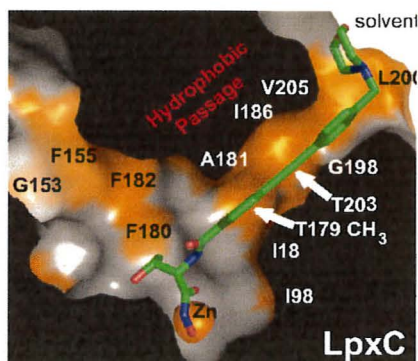


**Figure 3.** LpxC with CHIR-090 bound in active site.<sup>1</sup>

active site: a hydrophobic passage, a zinc ion, and a polar region (Figures 2 and 3).<sup>1</sup> Figure 2 shows palmitate and UDP in green bound in the LpxC active site of *A. aeolicus*.<sup>7</sup> Palmitate is bound in the hydrophobic passage (upper left), while UDP is bound in the polar region (lower right); the zinc ion is hidden

in the figure (upper middle region). Figure 3 shows the inhibitor CHIR-090 bound in the LpxC active site of *A. aeolicus*.<sup>1</sup> The hydrophobic passage has residues that contain R groups capable of dispersion forces, such as valine, isoleucine, alanine and glycine, and threonine (Figure 3).

Several inhibitors for LpxC have been developed and have provided significant progress toward the investigation of a novel, potent LpxC inhibitor. These inhibitors have led to the elucidation of the LpxC crystal structure and the critical residues and regions of the active site. Previous inhibitors (Figure 4) do not bind to all regions of the active site and have varying levels of activity against various strains of Gram-negative bacteria. A common feature among all of the inhibitors (Figure 4), except 1-68A, is the presence of a hydroxamic acid moiety (CONHOH). The hydroxamic acid moiety coordinates with the catalytic zinc present in the LpxC active site.<sup>8</sup> In addition, effective inhibitors contain a hydrophobic moiety, which occupies the hydrophobic passage of the active site. To interact with the hydrophobic passage, CHIR-090, BB-78485, and L-161,240 contain aromatic hydrophobic groups, while TU-514 contains a long hydrocarbon group. The

inhibitor CHIR-090 is shown bound to LpxC in the crystal structure (Figure 3). CHIR-090 interacts with LpxC in the hydrophobic passage and by binding with the zinc ion. However, the polar pocket of the LpxC active site is empty; hence, CHIR-090 does not take bind to all three regions in the active site. The inhibitor 1-68A interacts in the polar binding region and can successfully bind in the active site, which demonstrates the importance of developing novel targets that bind in the polar binding site in addition to the hydrophobic passage.<sup>9</sup> L-161,240, CHIR-090, and BB-78485 do not interact with the UDP binding site at all.<sup>9</sup>

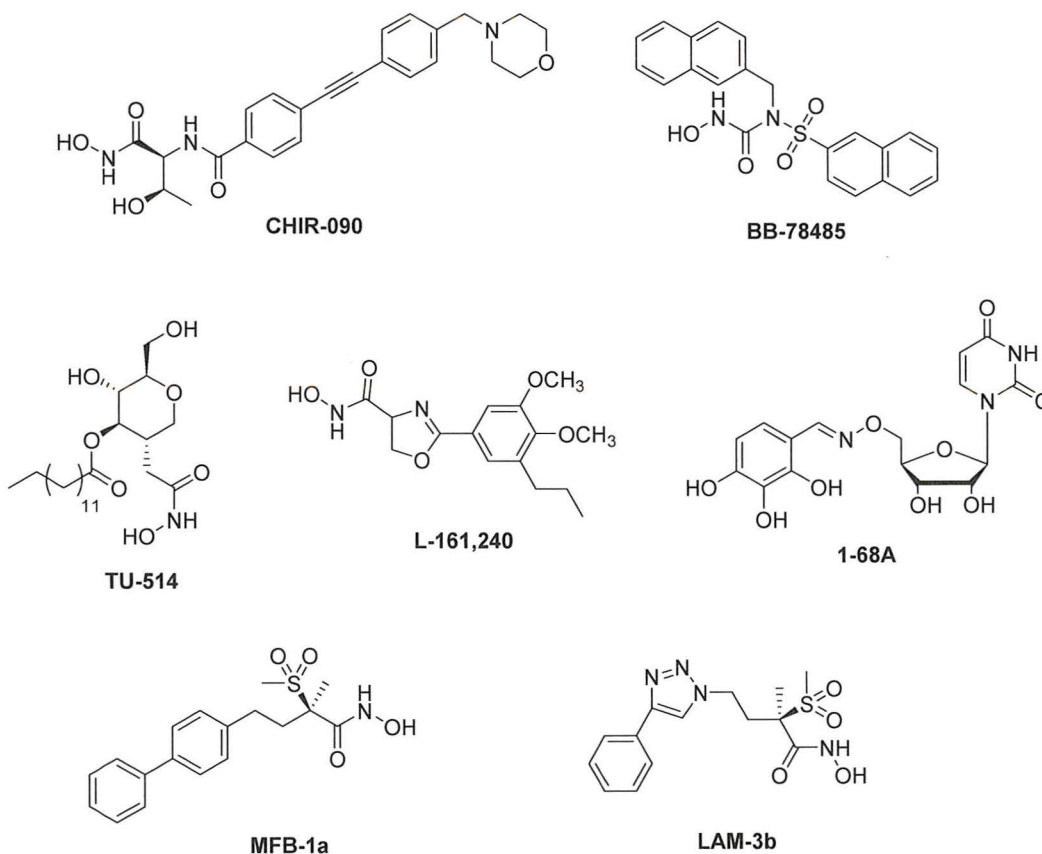


**Figure 4.** Previously developed inhibitors of LpxC.

Previous inhibitors have demonstrated limited-range activity against various strains of Gram-negative bacteria. LpxC orthologues differ in their sequence, with some degree of conservation. In comparison to *E. coli* LpxC, *P. aeruginosa*, *H. pylori*, *N. meningitidis*, and *R. leguminosarum* have the following sequence similarity: 57%, 43%, 49%, and 43%.<sup>6</sup> Although the strains of Gram-negative bacteria each have a slightly different LpxC, the conserved regions of the enzyme may allow for a broad-spectrum inhibitor if the ideal structure is determined. CHIR-090 has demonstrated potent activity against *E. coli*, *P. aeruginosa*, *H. pylori*, and *N. meningitidis*, but displays weak inhibitory activity against *R. leguminosarum*.<sup>1</sup> CHIR-090 does not take advantage of the polar region in the active site; if a moiety was added to interact in that region, it is possible that its activity would increase due to more binding interactions. The IC<sub>50</sub> values of the inhibitors from Figure 4 for *P. aeruginosa* are as follows: < 2.05 nM for CHIR-090, 1.37 nM for MFB-1a, and 0.85 nM for LAM-3b.<sup>10,11</sup> The IC<sub>50</sub> values in *E. coli* are 7.2 μM for TU-514, 0.023 μM for L-161,240, and 27 μM for 1-68A.<sup>9,12,13</sup>

### *C. Rationale and proposed design*

In order to develop an inhibitor of LpxC with broad-spectrum activity, compounds structurally different from previous inhibitors need to be designed to further investigate the critical interactions in the active site of LpxC. To accomplish this, a series of analogues will be synthesized and analyzed for their antibacterial activity; this will provide information about essential interactions and guide further inhibitor design. The long-term goal is to determine the essential interactions and design a potent, broad-spectrum inhibitor.

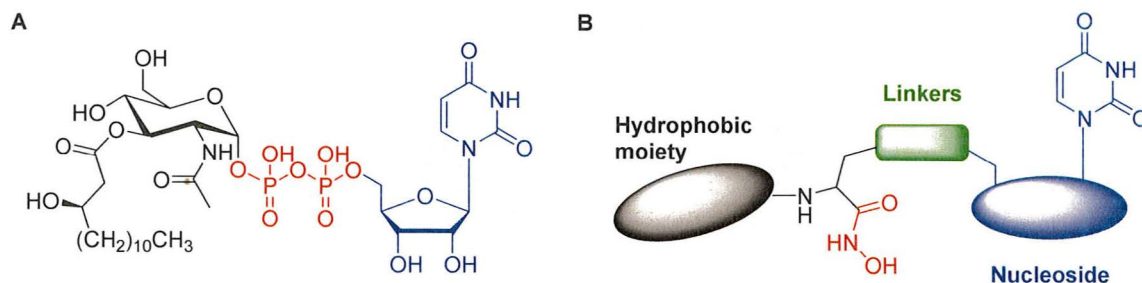


**Figure 5.** A) The structure of the natural substrate; B) The general structure of proposed analogues.

Our lab has previously worked on synthesizing natural substrate analogues to probe the active site of LpxC.<sup>14</sup> Information from previous inhibitors and the structure of the natural substrate influenced rational design for the analogue structures. The natural substrate features three regions: a hydrophobic moiety (black), a zinc-binding motif (red), and a uracil-based nucleoside (blue) (Figure 5A). Our analogues similarly feature a hydrophobic moiety, a hydroxamic acid moiety, and a uracil-based nucleoside (Figure 5B). In the LpxC active site, the hydrophobic moiety will fit into the hydrophobic passage, the hydroxamic acid moiety will bind to the zinc, and the nucleoside will bind in the polar region. The uracil-based nucleoside includes both the ribose and acyclic sugar nucleosides. The diphosphate was changed to a hydroxamic acid, which mimics the activity of the diphosphate to bind the zinc ion in the active site. The analogues are synthesized in two building blocks, the nucleoside block and the hydrophobic moiety with the hydroxamic acid block. The precursors are then coupled together with various linkers, such as a triazole linkage and ether linkage. The triazole linkage also binds well to zinc, which may strengthen binding in the active site.

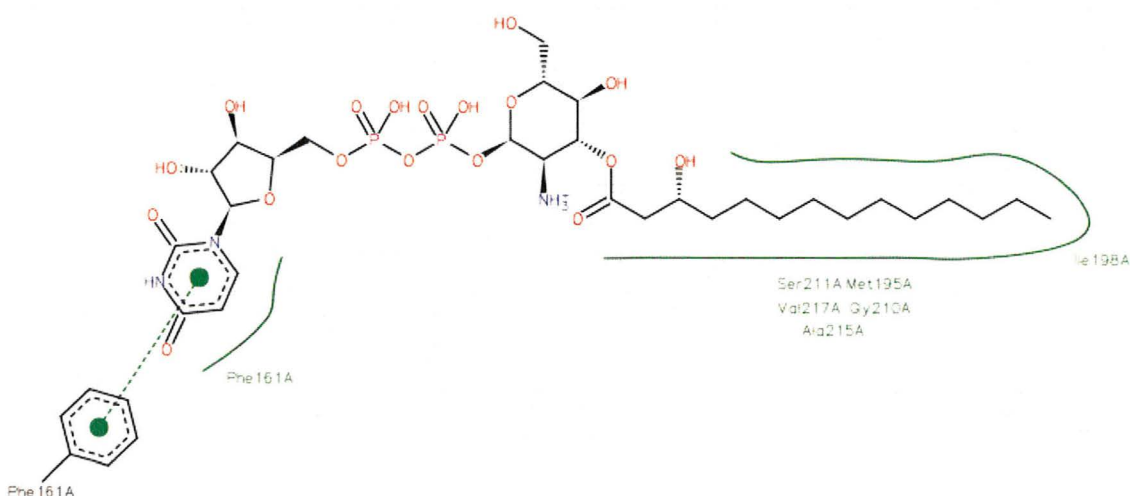


**Figure 6.** UDP-(3-O-(R-3-hydroxymyristoyl))-glucosamine bound in the LpxC active site with residues in polar region and hydrophobic pocket included (PDB 4MDT).<sup>13</sup>

Currently, a hydrophobic group is not being added to the analogues because of weak interactions present in that region of the active site. The hydrophobic passage has residues capable of dispersion forces, including Ser, Met, Val, Ala, and Gly.<sup>15</sup> UDP-(3-O-(R-3-hydroxymyristoyl))-glucosamine bound in LpxC of *E. coli* shows the residues found in the hydrophobic tunnel (Figure 6). There are no residues with  $\pi$  stacking abilities for stronger binding. However, analogues featuring a hydrophobic moiety, such as a biphenyl, will be synthesized in the future to compare to those compounds without a hydrophobic group. Previous inhibitors have demonstrated antibacterial activity when a biphenyl, or other hydrophobic moiety, is present.<sup>6</sup>

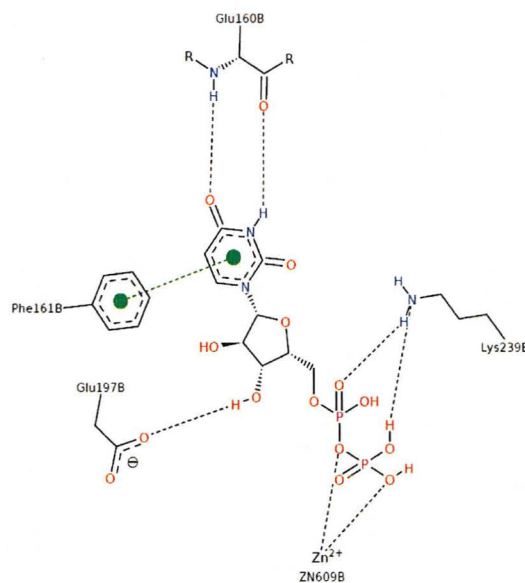


**Figure 7.** UDP bound in LpxC with important residues included (PDB 2IER).<sup>7</sup>



Despite the weaker interactions available in the hydrophobic pocket, there are stronger ones present in other regions of the active site. Figure 7 shows UDP bound in the active site in *A. aeolicus* to illustrate the interactions with the zinc ion and in the polar region (Figure 7).<sup>7</sup> There is  $\pi$  stacking between a Phe residue and uracil, as well as hydrogen bonding in various places by Glu and Lys. The zinc ion coordinates with the diphosphate, as mentioned previously, to further strengthen binding.

Previous work has focused on the synthesis of these two analogues (Figure 8). Both analogues feature a biphenyl group as the hydrophobic moiety, a hydroxamic acid moiety as the zinc-binding motif, and uridine as the nucleoside. The structures only differ in the linkage between the two building blocks, one containing a triazole linkage that is obtained via Cu-catalyzed azide-alkyne cycloaddition (Figure 8A), while the other contains an ether linkage obtained under basic conditions (Figure 8B).

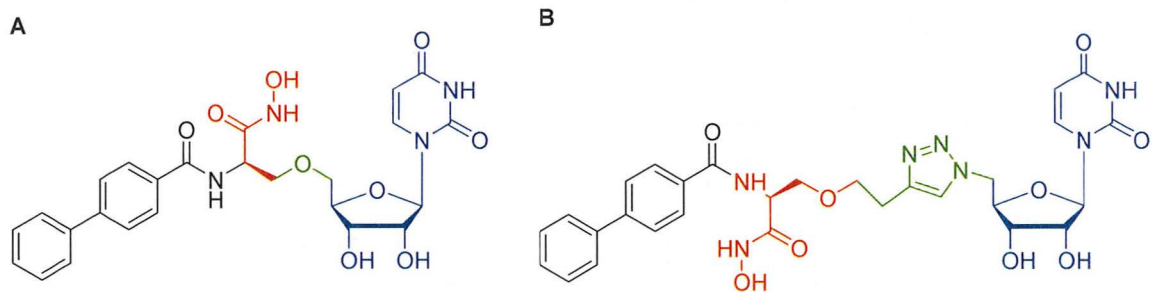


**Figure 8.** A) Triazole-linked analogue; B) Ether-linked analogue

#### D. Computational Studies

Preliminary docking studies by A. Katherine Hatstat and further computational studies by Allison J. L. Dewar have been completed to assess the potential inhibition activity of the analogues.<sup>16</sup> Analogues (Figure 9) were docked in the active site of LpxC from *A. aeolicus* (PDB ID: 2J65)<sup>17</sup> using ArgusLab (GADock Docking Engine and AScore scoring function), the most favorable pose was selected, and calculations between

residues and the ligand were completed for optimization.<sup>18</sup> Two molecules, SA-001 and SA-005, contain an ether linkage, while three molecules, SA-002, SA-003, and SA-004, contain a triazole linkage. In regard to the nucleoside, SA-001 and SA-005 have a modified, acyclic nucleoside, while the other three have a full ribose.

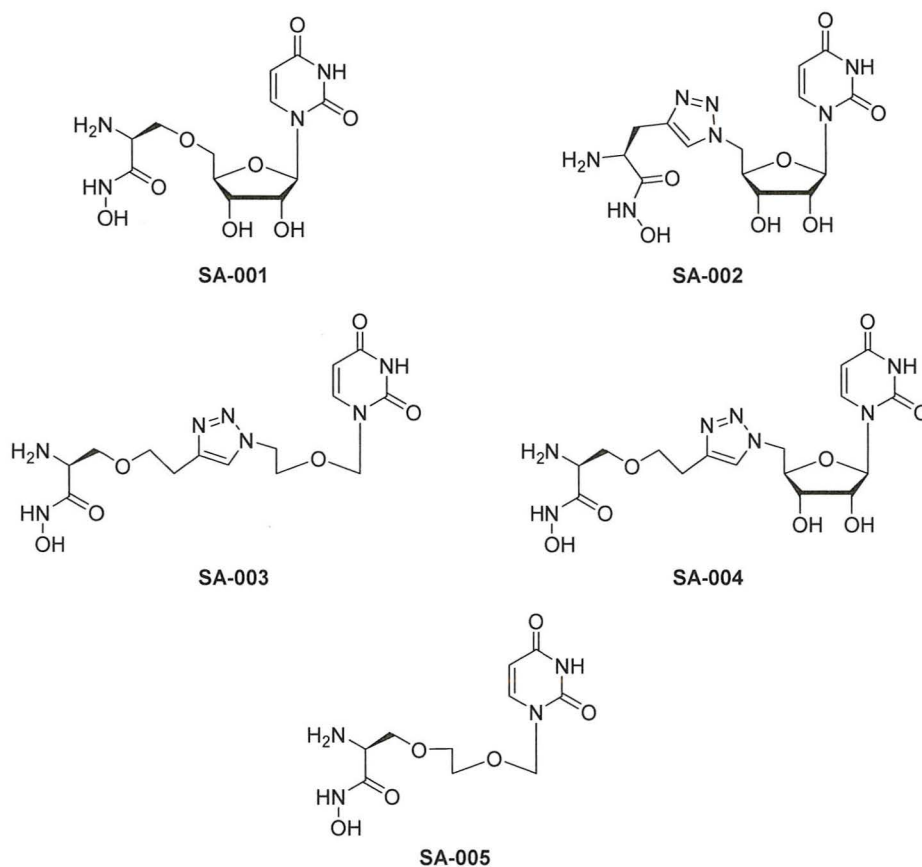


**Figure 9.** Structures of proposed natural substrate analogues.

Computational studies have demonstrated that SA-001 binds most weakly to LpxC compared to the other molecules, while SA-002 binds most tightly.<sup>16</sup> The triazole linkage is able to bind to the zinc ion, unlike the ether linkage. SA-002 binds more strongly than SA-003 and SA-004, which may be due to the shorter alkyne used in the triazole linkage. Comparing the acyclic sugar to the ribose, there is not a significant difference in the interaction energies between SA-003 and SA-004. However, SA-005

binds significantly stronger than SA-001, which may be due to the flexibility of the acyclic sugar as compared to the restricted flexibility of the ribose.

### *E. Purpose of thesis*

The goal of this work is to synthesize and characterize natural substrate analogue SA-002 (Figure 9). Analogues SA-001 and SA-004 have been synthesized to near completion, needing only the conversion of a carboxylic acid moiety to a hydroxamic acid moiety. Significant progress toward the synthesis of SA-003 and SA-005 has been made, but the final compounds have not been completed. SA-003 has been synthesized to the point of the triazole linkage with a carboxylic acid moiety, while SA-005 has been synthesized to the ether linkage with a carboxylic acid moiety (both missing the conversion to a hydroxamic acid moiety). Successful syntheses of all five analogues will allow for comparison of the importance of different groups for effective inhibition of LpxC.

## **II. Experimentals**

Unless otherwise indicated, all anhydrous solvents were commercially obtained and stored in Sure-seal bottles under argon. All other reagents and solvents were purchased as the highest grade available from Acros or Sigma-Aldrich and were used without further purification. Boc-L-Propargylglycine was purchased from Aurum Pharmatech. All moisture-sensitive reactions were carried out using dry solvents and under slight pressure of ultra-pure argon. Commercially available disposable syringes were used for transferring reagents and solvents. All single syntheses were conducted in

conventional flasks under an atmosphere of dry argon. The reaction to synthesize **13** was carried out in a glove bag under an atmosphere of argon. Proton ( $^1\text{H}$ ) and carbon ( $^{13}\text{C}$ ) NMR spectra were recorded on a Varian 400 MHz spectrometer. Chemical shifts ( $\delta$ ) are reported in parts per million (ppm) relative to  $\text{CHCl}_3$  at 7.26 or DMSO at 2.50 (for  $^1\text{H}$ ) and  $\text{CDCl}_3$  at 77.16 or DMSO at 39.52 (for  $^{13}\text{C}$ ). Coupling constants ( $J$ ) are reported in Hz throughout. Column chromatography was conducted using silica gel (Silicycle 55-65 Å).

*A. Ketal protection of uridine*

**1-((3aR,4R,6R,6aR)-6-(hydroxymethyl)-2,2-dimethyltetrahydrofuro[3,4-d][1,3]dioxol-4-yl)pyrimidine-2,4(1H,3H)-dione (1)**

Uridine (1.04 g, 4.1 mmol, 1 eq) was stirred in anhydrous acetone (50 mL, 0.082 mmol/mL) and treated with  $\text{H}_2\text{SO}_4$  (0.50 mL, 0.122 mmol/mL) drop-wise at rt. The resulting mixture was stirred at rt for 1.5 h. After 1.5 h, the reaction was neutralized with TEA (1.5 mL) and was concentrated under reduced pressure. The crude mixture was purified by silica gel column chromatography ( $\text{CH}_2\text{Cl}_2$ :MeOH, 0-8%) to afford alcohol **1** (997 mg, 86%) as a white solid.

$^1\text{H}$  NMR( $\text{CHCl}_3$ -*d*):  $\delta$  1.36 (s, 3 H) 1.58 (s, 3 H) 3.81 (dd,  $J = 12.1, 3.67$  Hz, 1 H) 3.92 (dd,  $J = 12.1, 2.69$  Hz, 1 H) 4.29 (q,  $J = 3.4$  Hz, 1 H) 4.96 (dd,  $J = 6.4, 3.45$  Hz, 1 H) 5.04 (dd,  $J = 6.4, 2.93$  Hz, 1 H) 5.61 (d,  $J = 2.9$  Hz, 1 H) 5.74 (d,  $J = 8.4$  Hz, 1 H) 7.41 (d,  $J = 8.0$  Hz, 1 H) 9.42 (br. s., 1 H)

$^{13}\text{C}$  NMR( $\text{CHCl}_3$ -*d*):  $\delta$  25.19, 27.15, 50.56, 62.38, 80.17, 80.42, 83.69, 86.83, 102.40, 114.30, 142.72, 150.44

*B. Synthesis of the ribose tosylate*

**((3aR,4R,6R,6aR)-6-(2,4-dioxo-3,4-dihydropyrimidin-1(2H)-yl)-2,2-dimethyltetrahydrofuro[3,4-d][1,3]dioxol-4-yl)methyl 4-methylbenzenesulfonate (2)**

Alcohol **1** (304 mg, 1.07 mmol, 1 eq) was co-evaporated with pyridine (2 x 2 mL) under Ar. Alcohol **1** was redissolved in CH<sub>2</sub>Cl<sub>2</sub> (5 mL) under Ar and pyridine (1 mL, 10. eq) was added. To the mixture was added Ts<sub>2</sub>O (549 mg, 1.68 mmol, 1.6 eq). The yellow solution was heated under reflux for 2 h and turned orange. After 2 h, the solution was diluted with CHCl<sub>3</sub> (20 mL) and washed with HCl (0.5 M, 3 x 5 mL) and saturated NaHCO<sub>3</sub> (3 x 5 mL). The organic layers were dried over Na<sub>2</sub>SO<sub>4</sub>, filtered, and concentrated under reduced pressure. The crude product was purified by silica gel column chromatography (Hex:EtOAc, 2:5, 1:3-1:5) to afford tosylate **2** (266 mg, 57%) as a pale yellow foam.

<sup>1</sup>H NMR (CHCl<sub>3</sub>-d): δ 1.31 (s, 3 H) 1.52 (s, 3 H) 2.41 (s, 3 H) 4.22 - 4.29 (m, 2 H) 4.29 - 4.35 (m, 1 H) 4.78 (dd, *J* = 6.4, 3.74 Hz, 1 H) 4.94 (dd, *J* = 6.4, 1.98 Hz, 1 H) 5.63 (d, *J* = 2.0 Hz, 1 H) 5.71 (d, *J* = 8.0 Hz, 1 H) 7.24 (d, *J* = 8.1 Hz, 1 H) 7.31 (d, *J* = 8.0 Hz, 2 H) 7.74 (d, *J* = 8.3 Hz, 2 H) 9.89 (s, 1 H)

*C. Synthesis of the ribose azide*

**1-((3aR,4R,6R,6aR)-6-(azidomethyl)-2,2-dimethyltetrahydrofuro[3,4-d][1,3]dioxol-4-yl)pyrimidine-2,4(1H,3H)-dione (5)**

Tosylate **2** (153 mg, 0.349 mmol, 1 eq) was dissolved in DMF (1 mL) under Ar. NaN<sub>3</sub> (110 mg, 1.69 mmol, 4.9 eq) was added to the solution. The reaction ran for 2 days (1<sup>st</sup>

day at room temperature, 2<sup>nd</sup> day at 45°C). The reaction mixture was concentrated under reduced pressure. The crude product was purified by silica gel column chromatography (CH<sub>2</sub>Cl<sub>2</sub>:MeOH, 0-20%) to afford azide **5** (103 mg, 96%) as a white solid.

<sup>1</sup>H NMR (CHCl<sub>3</sub>-*d*): δ 1.36 (s, 3 H) 1.57 (s, 3 H) 3.63 (d, *J* = 5.3 Hz, 2 H) 4.24 (q, *J* = 5.0 Hz, 1 H) 4.82 (dd, *J* = 6.5, 4.18 Hz, 1 H) 5.01 (dd, *J* = 6.5, 2.15 Hz, 1 H) 5.66 (d, *J* = 2.2 Hz, 1 H) 5.77 (d, *J* = 8.0 Hz, 1 H) 7.30 (d, *J* = 8.1 Hz, 1 H) 9.50 (br. s., 1 H)

*E. Synthesis of the ribose ether-linked carboxylic acid*

**N-(tert-butoxycarbonyl)-O-(((3aR,4R,6R,6aR)-6-(2,4-dioxo-3,4-dihydropyrimidin-1(2H)-yl)-2,2-dimethyltetrahydrofuro[3,4-d][1,3]dioxol-4-yl)methyl)-L-serine (**3**)**

Boc-Ser-OH (196 mg, 0.953 mmol, 2 eq) was dissolved in DMF (2 mL) under Ar. NaH (119 mg, 2.38 mmol, 5 eq) was added to solution at 0°C. The mixture was stirred for 30 min at 0°C, followed by stirring for 30 min at rt. Product **2** (157 mg, 0.477 mmol, 1 eq) was dissolved in DMF (1 mL) under Ar and added to the reaction mixture at 0°C. The mixture was stirred for 23 h. The reaction was stopped by the addition of water (4.5 mL) and acidified (pH 4) with HCl (1 M, ~0.5 mL). The crude product was extracted with Et<sub>2</sub>O (4 x 10 mL) and EtOAc (3 x 10 mL). The organic layers were combined, dried with MgSO<sub>4</sub>, filtered, and concentrated under reduced pressure to yield a solid (114 mg). The crude product was purified by silica gel column chromatography (CH<sub>2</sub>Cl<sub>2</sub>:MeOH, 100%, 95%:5%, 90%:10%) to afford ether-linked product **3** (81 mg, 48%) as a white solid.

<sup>1</sup>H NMR (CHCl<sub>3</sub>-*d*): δ 1.36 (s, 3 H) 1.45 (s, 5 H) 1.57 (s, 3 H) 3.77 - 3.87 (m, 1 H) 3.87 - 3.94 (m, 1 H) 4.00 - 4.07 (m, 1 H) 4.29 (q, *J* = 3.2 Hz, 1 H) 4.38 (br. s., 1 H) 4.94 (dd, *J* = 6.4, 3.45 Hz, 1 H) 5.01 (dd, *J* = 6.4, 2.84 Hz, 1 H) 5.64 (d, *J* = 2.8 Hz, 1 H) 5.75 (d, *J* =

8.0 Hz, 1 H) 7.47 (d,  $J = 8.0$  Hz, 1 H) 9.84 (br. s., 1 H)

$^{13}\text{C}$  NMR ( $\text{CHCl}_3$ - $d$ ):  $\delta$  25.11, 27.10, 28.21, 55.45, 62.20, 80.18, 83.84, 86.86, 94.68, 102.21, 114.23, 143.09, 150.46, 155.96, 164.38, 173.68

*F. Synthesis of the ribose triazole-linked carboxylic acid*

**N-(*tert*-butoxycarbonyl)-O-(2-(1-(((3aR,4R,6R,6aR)-6-(2,4-dioxo-3,4-dihydropyrimidin-1(2H)-yl)-2,2-dimethyltetrahydrofuro[3,4-d][1,3]dioxol-4-yl)methyl)-1H-1,2,3-triazol-4-yl)ethyl)-L-serine (6)**

Alkyne **4** (86 mg, 0.250 mmol, 1 eq) was dissolved in  $\text{CH}_3\text{CN}$  under Ar.  $\text{H}_2\text{O}$  (0.24 mL) was added to the solution. Azide **5** (98 mg, 0.317 mmol, 1 eq) was dissolved in  $\text{CH}_3\text{CN}$  (1.25 mL) and added to the reaction flask along with a Cu wire stir bar. The reaction was stirred overnight at  $35^\circ\text{C}$ , after the Cu wire was removed after 1.5 h. The reaction was monitored by TLC (1:1.5 Hex: EtOAc). Cu wire was added back in and the reaction was continued (50 h total). The reaction mixture was concentrated under reduced pressure. The crude product (blue-green foam) was purified by silica gel column chromatography ( $\text{CH}_2\text{Cl}_2$ :MeOH, 98%:2%, 95%:5%, 90%:10%) to afford triazole-linked product **6** (74 mg, 45%) as a white solid.

$^1\text{H}$  NMR ( $\text{CHCl}_3$ - $d$ ):  $\delta$  1.33 (s, 3 H) 1.42 (s, 8 H) 1.52 (s, 3 H) 2.99 (br. s., 1 H) 3.09 (br. s., 1 H) 3.47 (br. s., 2 H) 3.76 (s, 1 H) 4.03 (br. s., 1 H) 4.18 (br. s., 1 H) 4.32 (d,  $J=7.2$  Hz, 1 H) 4.47 (br. s., 1 H) 4.63 (br. s., 1 H) 4.70 (br. s., 1 H) 4.92 (br. s., 2 H) 5.01 - 5.21 (m, 1 H) 5.51 (br. s., 1 H) 5.75 (dd,  $J = 14.1, 7.85$  Hz, 2 H) 7.21 (d,  $J = 7.1$  Hz, 1 H) 10.27 (br. s., 1 H)

*G. Synthesis of acyclic uracil-based nucleoside***1-((2-hydroxyethoxy)methyl)pyrimidine-2,4(1H,3H)-dione (7)**

To a flask containing uracil (1.513 g, 13.5 mmol, 1 eq) was added CH<sub>3</sub>CN (34 mL, 0.393 mmol/mL) to form a suspension under Ar. At rt, bis(TMS)acetamide (9.25 mL, 37.8 mmol, 2.8 eq) was added slowly. After 1 h at rt, 1,3-dioxolane (1.0, 14.3 mmol, 1.03 eq), KI (2.218 g, 13.4 mmol, 0.994 eq) and TMSCl (2.4 mL, 18.9 mmol, 1.41 eq) were added to the clear solution at rt. After 16 h, the yellow, cloudy reaction mixture was quenched with MeOH (25 mL). The mixture turned white and was then neutralized with NaHCO<sub>3</sub> (5.122 g, added in 3 portions, 2 min apart). The solid was removed by filtration and the filtrate was concentrated under reduced pressure. The crude product was purified by silica gel column chromatography (EtOAc:MeOH, 90%:10%, 85%:15%, 80%:20%). The crystals formed in fractions were collected, while the liquid from the fractions was concentrated under reduced pressure. The non-crystalline solid was precipitated out with isopropanol. Purification yielded **7** as off-white solid (835 mg, 33%). R<sub>f</sub> of product: 0.44 in 4:1 EtOAc:MeOH.

<sup>1</sup>H NMR (DMSO-*d*<sub>6</sub>): δ 3.46 - 3.50 (m, 4 H) 5.08 (s, 2 H) 5.61 (d, *J* = 7.9 Hz, 1 H) 7.70 (d, *J* = 7.9 Hz, 1 H) 11.34 (s, 1 H)

*H. Synthesis of azide with acyclic sugar***2-((2,4-dioxo-3,4-dihydropyrimidin-1(2H)-yl)methoxy)ethyl 4-methylbenzenesulfonate (8)**

Acyclic sugar **7** (230 mg, 1.24 mmol, 1 eq) was co-evaporated with pyridine (3 x 2 mL) under Ar. Alcohol **7** was redissolved in pyridine (3.1 mL, 0.392 mmol/mL) under Ar and



Ts<sub>2</sub>O (640 mg, 1.96 mmol, 1.6 eq) was added at 0° C. The reaction ran for 4.5 h at 30° C. Then, the reaction mixture was diluted with CH<sub>2</sub>Cl<sub>2</sub> and washed with HCl (0.5 M, 4 x 7 mL), brine (3 x 3 mL), and saturated NaHCO<sub>3</sub> solution (2 x 7 mL). The organic layer was collected, dried with Na<sub>2</sub>SO<sub>4</sub>, and concentrated under reduced pressure. The crude product was purified by silica gel column chromatography (CH<sub>2</sub>Cl<sub>2</sub>:MeOH, 10%). The reaction afforded desired product **8** (95 mg, 23%) as a yellow solid. R<sub>f</sub> of product (0.75 in 9:1 CH<sub>2</sub>Cl<sub>2</sub>:MeOH).

<sup>1</sup>H NMR (CHCl<sub>3</sub>-*d*): δ 2.41 (s, 3 H) 3.76 (t, *J* = 4.4 Hz, 2 H) 4.11 (t, *J* = 4.5 Hz, 2 H) 5.10 (s, 2 H) 5.72 (d, *J* = 6.9 Hz, 1 H) 7.25 (d, *J* = 7.9 Hz, 1 H) 7.31 (d, *J* = 7.8 Hz, 2 H) 7.73 (d, *J* = 7.1 Hz, 2 H) 9.84 (br. s., 1 H)

<sup>13</sup>C NMR (CHCl<sub>3</sub>-*d*): δ ppm 21.58, 67.24, 68.55, 103.29, 127.81, 129.85, 132.52, 143.26, 145.04, 151.24, 163.69

#### **1-((2-azidoethoxy)methyl)pyrimidine-2,4(1H,3H)-dione (9)**

Tosylate **8** (253 mg, 0.743 mmol, 1 eq) was dissolved in DMF (1.8 mL) under Ar. NaN<sub>3</sub> (268 mg, 4.12 mmol, 4.86 eq) was added to the solution. The reaction was stirred for 15 h at 45 °C, after which time, the reaction was concentrated under reduced pressure. The crude product was purified by silica gel column chromatography (CH<sub>2</sub>Cl<sub>2</sub>:MeOH, 10%) to afford the desired product **9** (268 mg, not pure) as a white solid.

<sup>1</sup>H NMR (400 MHz, CHCl<sub>3</sub>-*d*): δ 3.40 - 3.44 (m, 5 H) 5.18 (d, *J* = 1.6 Hz, 2 H) 5.75 (dt, *J* = 7.9, 1.6 Hz, 1 H) 7.32 (d, *J* = 7.9 Hz, 1 H)

*I. Synthesis of the protected hydroxamic acid using Boc-L-propargylglycine*

***tert*-butyl ((2S)-1-oxo-1-(((tetrahydro-2H-pyran-2-yl)oxy)amino)pent-4-yn-2-yl)carbamate (12)**

In a round-bottom flask, Boc-L-propargylglycine (417 mg, 1.96 mmol, 1.0 eq) was measured out in a glove bag under an atmosphere of argon. To the alkyne was added CDMT (484 mg, 2.76 mmol, 1.4 eq) and THF (19 mL). At rt, NMM (0.35 mL, 3.183 mmol, 1.6 eq) was added, and the reaction mixture was stirred. After 1.5 h, THP-O-NH<sub>2</sub> (373 mg, 3.18 mmol, 1.6 eq) was added. After 19.5 h, the reaction mixture was filtered through celite (~2 inches). The celite was rinsed with CH<sub>2</sub>Cl<sub>2</sub>. The resulting solution was concentrated and purified by silica gel column chromatography (CH<sub>2</sub>Cl<sub>2</sub>:MeOH, 5%) to yield a cleaner product that was further purified with another column (Hex:EtOAc 1:4) to afford **12** as a white solid (761 mg). R<sub>f</sub> of product 0.71-0.74 1:4 Hex:EtOAc.

<sup>1</sup>H NMR (CHCl<sub>3</sub>-*d*): δ 1.38 (s, 9 H) 1.46 - 1.63 (m, 4 H) 1.68 - 1.83 (m, 4 H) 2.60 (br. s., 2 H) 3.55 (d, *J* = 11.0 Hz, 1 H) 3.91 (s, 2 H) 4.28 (t, *J* = 7.0 Hz, 1 H) 4.92 (d, *J* = 2.5 Hz, 1 H) 5.54 (d, *J* = 7.7 Hz, 1 H) 9.96 (br. s., 1 H)

*J. Synthesis of acyclic triazole-linked carboxylic acid using alkylated Boc-L-Ser (SA-003)*

***N*-(*tert*-butoxycarbonyl)-O-(2-(1-(2-((2,4-dioxo-3,4-dihydropyrimidin-1(2H)-yl)methoxy)ethyl)-1H-1,2,3-triazol-4-yl)ethyl)-L-serine (10)**

In a 5 mL round bottom flask, azide **9** (103 mg, 0.488 mmol, 1 eq) was added. To azide **9** was added alkyne **4** (92 mg, 0.358 mmol, 1 eq) dissolved in CH<sub>3</sub>CN (0.7 mL). The alkyne container was rinsed with CH<sub>3</sub>CN (0.5 mL) and added to the reaction flask. To the flask was added water (0.4 mL, 1.74 mmol/mL) and Cu powder (9 mg, 0.142 mmol, 0.36

eq). The reaction was sonicated for 10 min before being stirred at 35 °C overnight. At 21 h, a second addition of Cu powder (4 mg, 0.063 mmol) was added. The reaction flask was sonicated for 10 min and stirred at 35 °C. At 24 h, the reaction was concentrated under reduced pressure. The crude product was purified by column chromatography (CH<sub>2</sub>Cl<sub>2</sub>:MeOH, 5%) to afford the desired product as a solid (112 mg, 69%). R<sub>f</sub> for product (0.379 in 9:1 CH<sub>2</sub>Cl<sub>2</sub>:MeOH).

<sup>1</sup>H NMR (CHCl<sub>3</sub>-*d*): δ 1.43 (s, 9 H) 2.95 - 3.17 (m, 2 H) 3.79 (d, *J* = 10.8 Hz, 1 H) 4.01 (t, *J* = 4.8 Hz, 2 H) 4.15 - 4.27 (m, 1 H) 4.35 (d, *J* = 8.1 Hz, 1 H) 4.52 (t, *J* = 4.8 Hz, 2 H) 4.56 - 4.66 (m, 1 H) 4.76 (br. s., 1 H) 5.11 (s, 2 H) 5.30 (d, *J* = 1.4 Hz, 2 H) 5.69 - 5.78 (m, 2 H) 7.25 (dd, *J* = 7.9, 1.17 Hz, 1 H) 7.57 (s, 1 H) 9.81 (br. s., 1 H)

*K. Synthesis of acyclic ether-linked carboxylic acid (SA-005)*

**N-(tert-butoxycarbonyl)-O-(2-((2,4-dioxo-3,4-dihydropyrimidin-1(2H)-yl)methoxy)ethyl)-L-serine (11)**

In a round-bottom flask, NaH (60% in oil, 85 mg, 3.54 mmol, 4.5 eq) was dissolved in DMF (1 mL) under Ar. In another flask, Boc-L-Ser (215 mg, 1.05 mmol, 2 eq) was dissolved in DMF (2 mL) under Ar. At 0 °C, the Boc-L-Ser solution was added slowly to NaH. The mixture was warmed to rt and stirred for 1 h. After 1 h at 0 °C, toylate **8** (168 mg, 0.494 mmol, 1 eq) in DMF (1 mL) was added slowly. The reaction stirred at 0 °C for 10 min before the ice bath was removed. At 3 h, the excess NaH was quenched with NH<sub>4</sub><sup>+</sup>Cl<sup>-</sup> solution, and the reaction was concentrated under reduced pressure. At 0°C, water (2 mL) was added to the residue. The mixture was acidified with HCl (3 M) to pH <3. The product was extracted from the aqueous mixture with EtOAc (4 x 5 mL), dried

with MgSO<sub>4</sub>, filtered, and concentrated under reduced pressure. The crude product was purified by silica gel column chromatography (CH<sub>2</sub>Cl<sub>2</sub>:MeOH, 10%) to afford product **11** as a white solid (~100 mg).

<sup>1</sup>H NMR (CHCl<sub>3</sub>-*d*): δ 1.38 (s, 25 H) 3.54 - 3.65 (m, 4 H) 3.65 - 3.72 (m, 2 H) 3.73 - 3.79 (m, 1 H) 3.85 (dd, *J* = 10.2, 4.77 Hz, 3 H) 4.06 (q, *J* = 5.4 Hz, 2 H) 4.16 (dt, *J* = 7.0, 3.33 Hz, 1 H) 5.16 (q, *J* = 10.3 Hz, 2 H) 5.68 (d, *J* = 8.2 Hz, 1 H) 5.73 (d, *J* = 6.6 Hz, 2 H) 7.45 (d, *J* = 7.9 Hz, 1 H)

*L. Synthesis of ribose triazole-linked protected hydroxamic acid using propargylglycine (SA-002)*

***tert*-Butyl ((2S)-3-(1-(((3aR,4R,6R,6aR)-6-(2,4-dioxo-3,4-dihydropyrimidin-1(2H)-yl)-2,2-dimethyltetrahydrofuro[3,4-d][1,3]dioxol-4-yl)methyl)-1H-1,2,3-triazol-4-yl)-1-oxo-1-(((tetrahydro-2H-pyran-2-yl)oxy)amino)propan-2-yl)carbamate (13)**

To alkyne **12** (149 mg, 0.477 mmol, 1 eq) was added azide **5** (155 mg, 0.501 mmol, eq) dissolved in CH<sub>3</sub>CN (2 mL). The azide container was rinsed with CH<sub>3</sub>CN (1.4 mL) and added to the reaction flask. Water (0.6 mL) and Cu powder (13 mg, 0.205 mmol, 0.36 eq) were added at rt. The reaction was sonicated for 10 min before stirring at 35 °C overnight. After 21 h, the reaction was concentrated under reduced pressure. The green crude product was purified by silica gel column chromatography (CH<sub>2</sub>Cl<sub>2</sub>:MeOH 5%) to afford the desired product as a solid (225 mg, 76%).

<sup>1</sup>H NMR (CHCl<sub>3</sub>-*d*): δ 1.30 (br. s., 3 H) 1.37 (br. s., 8 H) 1.50 (br. s., 6 H) 1.72 (br. s., 3 H) 3.12 (br. s., 1 H) 3.54 (br. s., 1 H) 3.91 (d, *J* = 8.8 Hz, 1 H) 4.41 (br. s., 1 H) 4.67 (br.

s., 1 H) 4.86 (br. s., 1 H) 5.02 (br. s., 1 H) 5.54 (d,  $J = 10.2$  Hz, 1 H) 5.71 (br. s., 1 H) 5.82 (br. s., 1 H) 7.16 (br. s., 1 H) 7.43 - 7.66 (m, 1 H) 10.24 - 10.47 (m, 1 H)

**(S)-2-amino-3-(1-(((2R,3S,4R,5R)-5-(2,4-dioxo-3,4-dihydropyrimidin-1(2H)-yl)-3,4-dihydroxytetrahydrofuran-2-yl)methyl)-1H-1,2,3-triazol-4-yl)-N-hydroxypropanamide (14)**

In a round-bottom flask, TFA (1 mL) was added to **13** (187 mg, 0.301 mmol) dissolved in  $\text{CH}_2\text{Cl}_2$  (1 mL) at 0 °C. After 14.5 h, reaction was stopped and concentrated. The residue was rinsed with  $\text{CH}_2\text{Cl}_2$  and concentrated. The residue was dissolved in MeOH and precipitated out with  $\text{Et}_2\text{O}$  to yield an off-white solid (130 mg). In a round-bottom flask,  $\text{H}_2\text{O}$  (3 mL, 10% in TFA) was added to the partially-deprotected product with the ketal protecting group remaining (111 mg, 0.254 mmol) at 0 °C. After 1 h, the reaction was stopped and concentrated. The residue was rinsed with  $\text{CH}_2\text{Cl}_2$  and concentrated. The residue was dissolved in MeOH and precipitated by the addition of  $\text{Et}_2\text{O}$  to yield product **14** as an off-white solid (99 mg, 83%).

$^1\text{H}$  NMR ( $\text{DMSO}-d_6$ ):  $\delta$  3.04 (dd,  $J = 15.0, 7.19$  Hz, 1 H) 3.11 (dd,  $J = 15.0, 6.75$  Hz, 1 H) 3.85 (t,  $J = 7.0$  Hz, 1 H) 3.96 (q,  $J = 5.2$  Hz, 1 H) 4.12 (quin,  $J = 5.1$  Hz, 2 H) 4.63 (dd,  $J = 14.5, 7.68$  Hz, 1 H) 4.70 (dd,  $J = 14.5, 4.06$  Hz, 1 H) 5.41 (d,  $J = 5.5$  Hz, 1 H) 5.57 (d,  $J = 5.5$  Hz, 1 H) 5.66 (d,  $J = 8.0$  Hz, 1 H) 5.74 (d,  $J = 5.2$  Hz, 1 H) 7.57 (d,  $J = 8.1$  Hz, 1 H) 7.86 (s, 1 H) 9.30 (s, 1 H)

### III. Results and Discussion

#### *A. Synthesis of ribose ether-linked carboxylic acid analogue (SA-001)*

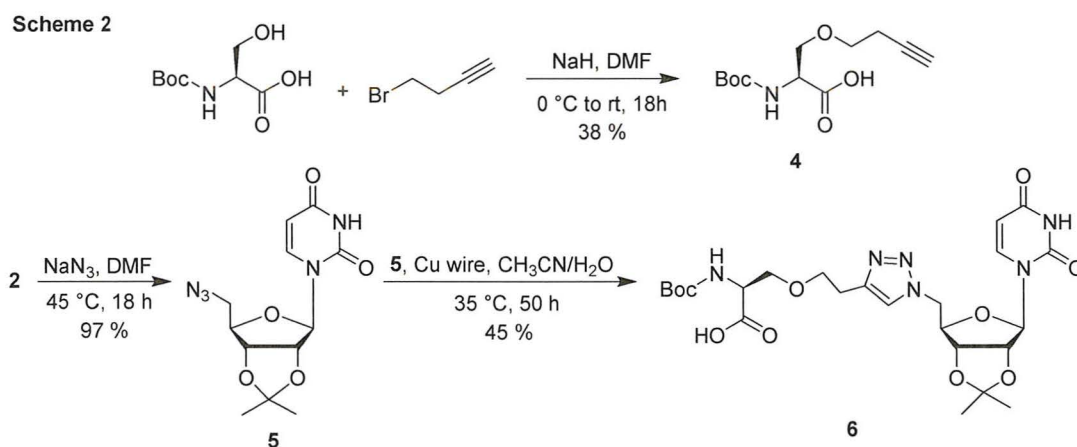
Synthesis of the ribose ether-linked analogue began with a ketal protection of the 2'- and 3'-hydroxyl groups on uridine to produce **1**, followed by the activation of the 5'-hydroxyl group to a tosyl group in **2** (Scheme 1) according to the literature procedures.<sup>19,20</sup> The ketal protection proceeds with ease, attaining a high yield of 91%, as compared to the literature yield of 100%.<sup>19</sup> However, the tosylation reaction proceeds with some difficulty.

There are literature procedures describing the use of either tosyl anhydride (Ts<sub>2</sub>O) or tosyl chloride (TsCl) have both been used with pyridine, as well as the presence or absence of dichloromethane.<sup>20,21</sup> Various reaction conditions have been attempted to determine the optimal conditions to produce a pure product in a high yield, including running the reaction for 2-4 hours or overnight, or at room temperature or slightly heated. Despite Winans and colleagues reporting a 98% yield on the formation of the tosylate, only a maximum of 67% yield has been observed. The aqueous work up with dilute hydrochloric acid, brine, and saturated sodium bicarbonate solution could be affecting the product, as the organic and aqueous phases do not separate very well and seem to emulsify. Another plausible explanation for lower yields is the use of silica gel column chromatography to purify the tosylate, as the tosylate product may interact with the slightly acidic silica gel, resulting in destroying the product. However, Winans and coworkers purified their tosylate by column chromatography without issue.

In order to synthesize the ether linkage, the tosylate was coupled with commercially available Boc-L-Ser using sodium hydride in dimethylformamide, resulting



a yield of 38%. The reaction conditions, as well as the equivalents of reagents, have been altered, but better conditions resulting in higher yields have yet to be determined. Despite the challenges of the alkylation to form the azide, the triazole linkage has worked with ease. In the first attempt to couple the azide and alkyne together, a copper wire-wrapped stir bar was utilized, and the reaction ran 48 h to provide a product in a 45% yield.<sup>23</sup> However, the yield was increased to 76% when copper powder was used, and the reaction was sonicated for 10 min before stirring overnight.



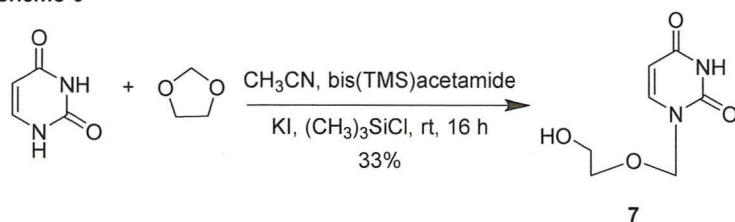
### C. Synthesis of acyclic nucleoside

To synthesize the acyclic nucleoside, uracil was reacted with 1,3-dioxolane to produce compound 7 according to the published procedure (Scheme 3).<sup>24</sup> Initial attempts at this synthesis were unsuccessful in obtaining product. However, when equivalents were adjusted for the reagents, the reaction proceeded. The bis(TMS)acetamide was changed from 2.2 eq to 2.82 eq., the chlorotrimethylsilane was changed from 1.0 eq. to 1.41 eq., and the acetonitrile was changed from 0.67 mmol/mL to 0.393 mmol/mL for uracil. In addition, during the purification by column chromatography, crystals were observed in the fractions. After analyzing the crystals by NMR, they were determined to



be the actual product. Multiple literature procedures were explored to determine the best conditions and equivalents; that being said, the yields for all reviewed literature were around 30%.<sup>24-27</sup> Hence, even though compound **7** was produced in 33%, the yield is comparable to that of the literature.

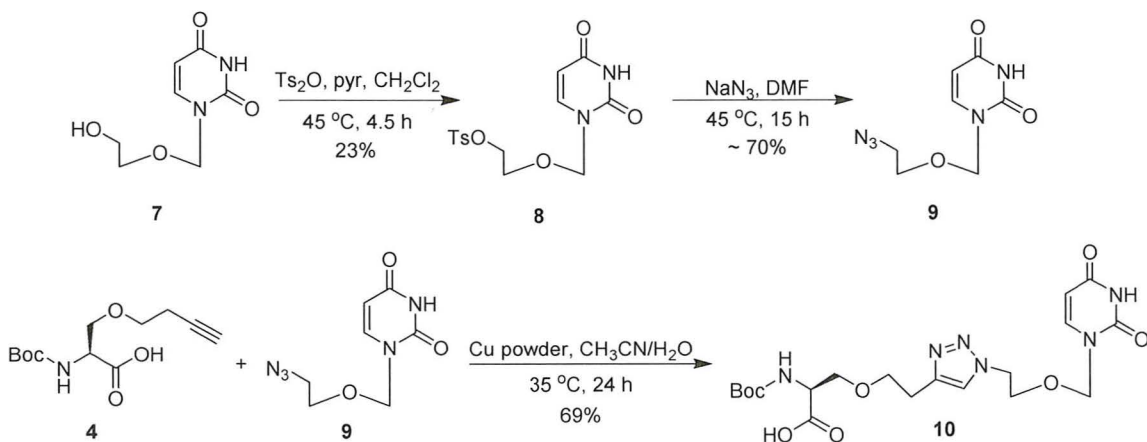
Scheme 3



#### D. Synthesis of acyclic triazole-linked carboxylic acid using alkylated Boc-L-Ser (SA-003)

Synthesis of the acyclic triazole-linked analogue featuring the alkylated Boc-L-Ser to the carboxylic acid **4** is illustrated in Scheme 3. The acyclic nucleoside **7** was tosylated in **8**, followed by exchanging the tosylate for an azide **9** using methods described earlier (Schemes 1 and 2).<sup>20</sup> The commercially available Boc-L-Ser was alkylated to produce **5d** (Scheme 2).<sup>22</sup> Azide **9** and alkyne **5** were coupled together to form the triazole linkage in **10**.<sup>23</sup>

Scheme 4



Tosylation of the acyclic nucleoside proved to be difficult, just as the tosylation of the ribose was challenging. Various attempts to synthesize the acyclic tosylate are described in Table 1. The literature was reviewed to find the best reaction conditions, but those have yet to be determined.<sup>20,28-30</sup> Both TsCl and Ts<sub>2</sub>O have been used, as well as the presence or absence of an aqueous workup. Trial 3 provided pure product with a yield of 23% and a clean <sup>1</sup>H NMR. However, the tosylate from experiment 3 was not used when the tosylate was converted to an azide, but rather the tosylate from trial 5 was used. This tosylate was not obtained as a pure compound before taking it into the next reaction, which means both the tosylation and azide reactions do not have yields. The tosylate formed in experiment 5 may have also undergone side reactions. The reaction may have run too long, and the compound dimerized, since the tosylate is easily displaced.

**Table 1. Reagents and results for the formation of the acyclic tosylate**

Exp	Reagents	Reaction Conditions	Workup and purification	Result
1	7, TsCl, pyr	0° C to rt, 16 h	Added MeOH, Conc. Column 1: CH <sub>2</sub> Cl <sub>2</sub> :MeOH Column 2: Hex:EtoAc	12%
2	7, TsCl, pyr	0° C to rt, 17.25 h	Diluted with CH <sub>2</sub> Cl <sub>2</sub> Wash: HCl, brine Column: CH <sub>2</sub> Cl <sub>2</sub> :MeOH	9%
3	7, Ts <sub>2</sub> O, pyr	0° C to 35° C, 4.5 h	Diluted with CH <sub>2</sub> Cl <sub>2</sub> Wash: HCl, brine, NaHCO <sub>3</sub> Column: CH <sub>2</sub> Cl <sub>2</sub> :MeOH	23%
4	7, Ts <sub>2</sub> O, pyr	0° C to rt, 16.5 h	Diluted with CH <sub>2</sub> Cl <sub>2</sub> Wash: HCl, brine, NaHCO <sub>3</sub>	0%
5	7, TsCl, pyr	0° C to rt, 14.75 h	Conc. Column 1: CH <sub>2</sub> Cl <sub>2</sub> :MeOH Column 2: CH <sub>2</sub> Cl <sub>2</sub> :MeOH	56%, impure

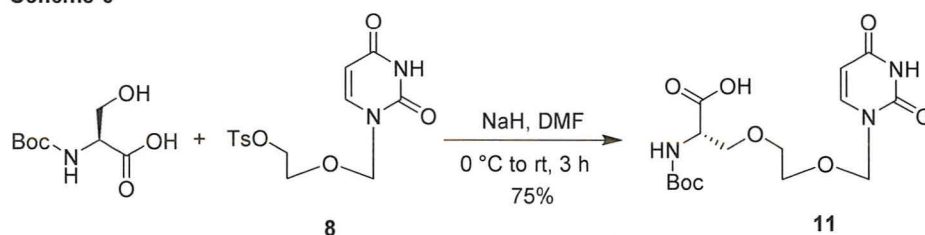
The synthesis of **9** has only been performed once (Scheme 4). As mentioned above, impure tosylate was used. The azide reaction proceeded with success to ~70%

yield, even though there was material unable to react to form the azide. Compound **9** could not be purified by silica gel column chromatography from the by-products. Despite the difficulty in purification, the azide was taken to the next step to form the triazole linkage. The CuCAAC proceeded with a 69% yield, which is comparable to the 76% yield for the ribose triazole-linked carboxylic acid **6**. Silica gel column chromatography eluded a pure compound, despite the impurities present in the azide.

#### E. Synthesis of acyclic ether-linked carboxylic acid (SA-005)

The synthesis of the ether-linked analogue began with synthesizing acyclic tosylate **8** as discussed previously (Scheme 4).<sup>20</sup> Commercially-available Boc-L-Ser was coupled with **3** under basic conditions to produce the ether linkage in **6** (Scheme 5).<sup>10</sup>

**Scheme 5**



#### F. Conversion of carboxylic acid to hydroxamic acid

Converting the carboxylic acid (COOH) to the hydroxamic acid (CONHOH) has proven to be the most challenging obstacle so far. Compounds SA-001, SA-003, and SA-004 still need the carboxylic acid to be converted to the hydroxamic acid. Given the small amount of each carboxylic acid analogue that has been synthesized, several ‘practice’ reactions have been performed to test the success of the conversion, some of which are found in Table 2. Instead of using **3**, **6**, or **10**, Boc-L-Ser-CO<sub>2</sub>H and biphenyl-CO<sub>2</sub>H were

purchased, and Boc-D-Ser-CO<sub>2</sub>H was made from D-Ser using Boc<sub>2</sub>O. Five methods have been tested (Table 2). The method using DCC has worked successfully in 67% of the reactions, of which both successful reactions utilized a commercially available carboxylic acid.<sup>31</sup> Using DCC as a coupling agent was preferable because of the high yields and ease of the reaction, due to the precipitation of the urea by-product. However, due to the inconsistencies between using reagents from different sources, the use of DCC was abandoned. A possible explanation to the difficulty in converting the carboxylic acid moiety to the hydroxamic acid moiety is the presence or absence of the proton on the hydroxyl group of the carboxylic acid. The proton is present in the commercially available carboxylic acid starting materials, but may be absent in the synthesized carboxylic acids. This would account for the difficulty in converting analogues SA-001, SA-003, SA-004, and SA-005 to the hydroxamic acid, as the synthesis of the carboxylic acid precursors required basic conditions i.e., the ether linkage was performed under basic conditions, while both triazole-linked analogues utilized an alkyne that was made under basic conditions.

In attempt to find another method for the formation of the hydroxamic acid, EDC and PyBOP were utilized as coupling reagents (Table 2).<sup>10</sup> Neither of the reactions proceeded at all, so both methods were abandoned.

The fourth method tried used was TCT, or cyanuric chloride.<sup>32</sup> The first reaction using TCT (Table 2, entry 5) was successful in making the hydroxamic acid. However, three additional reactions were performed with TCT using Boc-L-Ser-CO<sub>2</sub>H and biphenyl-CO<sub>2</sub>H that all resulted in no reaction. The TCT was exposed to the air during experimentation, allowing it to react with moisture and hence, inactivating it. Due to the

success of the first TCT reaction, 2-chloro-4,6-dimethoxy-1,3,5-triazine (CDMT), a similar reagent to TCT, was used. CDMT has one chlorine atom and two methoxy groups as opposed to the three chlorine groups in TCT. As a new strategy, Boc-L-Propargylglycine was purchased to use as the amino acid and to make the hydroxamic acid. Using the CDMT as a coupling reagent, a hydroxamic acid was successfully synthesized in a high yield.<sup>10</sup>

**Table 2. Reagents and results for the attempted conversion of the carboxylic acid to the hydroxamic acid**

Exp	Carboxylic Acid	Hydroxyl Amine	Method	Result
1	Boc-L-Ser-CO <sub>2</sub> H	THP-O-NH <sub>2</sub>	DCC, CH <sub>2</sub> Cl <sub>2</sub>	94%
2	Biphenyl-CO <sub>2</sub> H	TMS-O-NH <sub>2</sub>	HOBt, EDC, TEA, CH <sub>2</sub> Cl <sub>2</sub>	NR
3	Biphenyl-CO <sub>2</sub> H	TMS-O-NH <sub>2</sub>	PyBOP, DIPEA, CH <sub>2</sub> Cl <sub>2</sub>	NR
4	Biphenyl-CO <sub>2</sub> H	TBDMS-O-NH <sub>2</sub>	DCC, CH <sub>2</sub> Cl <sub>2</sub>	85%
5	Biphenyl-CO <sub>2</sub> H	TBDMS-O-NH <sub>2</sub>	TCT, NMM, DMAP, CH <sub>2</sub> Cl <sub>2</sub>	~30%
6	Boc-D-Ser-CO <sub>2</sub> H	TBDMS-O-NH <sub>2</sub>	DCC, CH <sub>2</sub> Cl <sub>2</sub>	NR
7	Boc-L-propargylglycine	THP-O-NH <sub>2</sub>	CDMT, NMM, THF	--

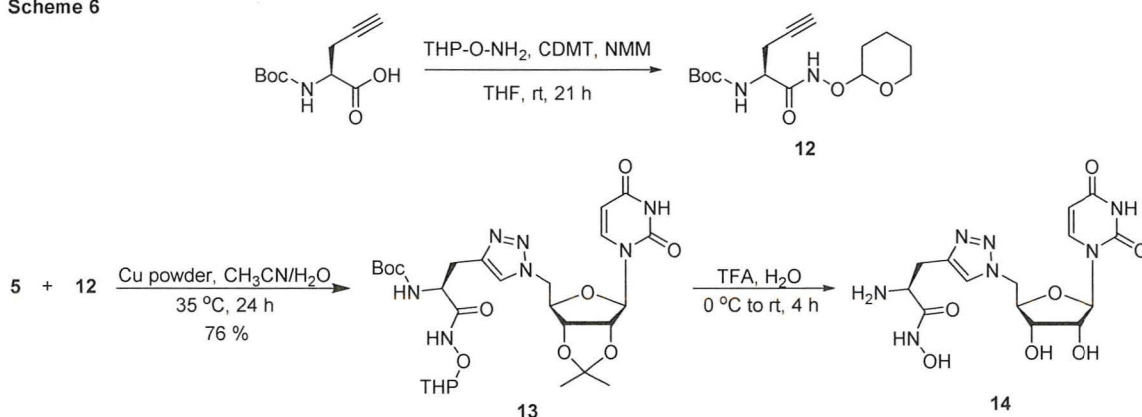
*G. Synthesis of acyclic triazole-linked protected hydroxamic acid using propargylglycine (SA-002)*

As mentioned in the previous section, the formation of the hydroxamic acid from the carboxylic acid has proven to be fairly difficult. Using commercially available Boc-L-propargylglycine bypassed the difficult alkylation of Boc-L-Ser and ensured that the proton on the carboxylic acid was present. A protected hydroxamic acid was successfully added to the Boc-L-propargylglycine using CDMT, which was then easily coupled with ribose azide **5**.

The new strategy (Scheme 6) of synthesizing a triazole-linked analogue began with the conversion of the carboxylic acid of the Boc-L-propargylglycine to a protected

hydroxamic acid **12**.<sup>12</sup> Azide **5** was made according to established literature (Scheme 2).<sup>20</sup> Then, alkyne **12** and azide **5** were coupled together via CuCAAC to yield **13**. A final reaction to deprotect the amino groups and the 2'- and 3'-hydroxyl groups was performed to yield **14**, the final analogue SA-002, as confirmed by <sup>1</sup>H NMR. A deprotection reaction using TFA and CH<sub>2</sub>Cl<sub>2</sub> was attempted prior to using TFA and water. However, without the water, only the Boc and THP protecting groups were removed, while the ketal protecting group remained. After realizing that water was needed as a nucleophile to remove the ketal protecting group, a second deprotection reaction was performed to successfully yield the completed SA-002 compound.

Scheme 6



#### IV. Conclusion

We have successfully synthesized twelve intermediates, making progress toward the complete synthesis of all five analogues. Of the five analogues, SA-002 has been successfully completed in seven steps. This work focuses on the synthesis of natural substrate analogues featuring an acyclic sugar, as well as developments toward the successful conversion of a carboxylic acid to a hydroxamic acid. The method using CDMT as a coupling agent seems to work the best in converting the carboxylic acid to the hydroxamic acid.

## V. References

- (1) Barb, A. W.; Jiang, L.; Raetz, C. R. H.; Zhou, P. Structure of the deacetylase LpxC bound to the antibiotic CHIR-090: Time-dependent inhibition and specificity in ligand binding. *Proc. Natl. Acad. Sci. U. S. A.* **2007**, *104*, 18433-18438.
- (2) Mansoor, U. F.; Reddy, P. A. Hydantoin derivatives useful as antibacterial agents. Application: PCT60/841,883 Patent.
- (3) Levy, S. B. Antibiotic resistance - the problem intensifies. *Adv. Drug Delivery Rev.* **2005**, *57*, 1446-1450.
- (4) Pollack, A. Bacteria are bad news. *The New York Times*, February 27, 2010, 2010.
- (5) Barb, A. W.; Zhou, P. Mechanism and inhibition of LpxC: An essential zinc-dependent deacetylase of bacterial lipid a synthesis. *Curr. Pharm. Biotechnol.* **2008**, *9*, 9-15.
- (6) Barb, A. W.; McClerren, A. L.; Snehelatha, K.; Reynolds, C. M.; Zhou, P.; Raetz, C. R. H. Inhibition of lipid A biosynthesis as the primary mechanism of CHIR-090 antibiotic activity in *Escherichia coli*. *Biochemistry* **2007**, *46*, 3793-3802.
- (7) Gennadios, H. A.; Christianson, D. W. Binding of Uridine 5'-Diphosphate in the "Basic Patch" of the Zinc Deacetylase LpxC and Implications for Substrate Binding. *Biochemistry* **2006**, *45*, 15216-15223.
- (8) Gennadios, H. A.; Whittington, D. A.; Li, X.; Fierke, C. A.; Christianson, D. W. Mechanistic Inferences from the Binding of Ligands to LpxC, a Metal-Dependent Deacetylase. *Biochemistry* **2006**, *45*, 7940-7948.

(9) Barb, A. W.; Leavy, T. M.; Robins, L. I.; Guan, Z. Q.; Six, D. A.; Zhou, P.; Bertozzi, C. R.; Raetz, C. R. H. Uridine-Based Inhibitors as New Leads for Antibiotics Targeting Escherichia coli LpxC. *Biochemistry* **2009**, *48*, 3068-3077.

(10) Brown, M. F.; Reilly, U.; Abramite, J. A.; Arcari, J. T.; Oliver, R.; Barham, R. A.; Che, Y.; Chen, J. M.; Collantes, E. M.; Chung, S. W.; Desbonnet, C.; Doty, J.; Doroski, M.; Engtrakul, J. J.; Harris, T. M.; Huband, M.; Knafels, J. D.; Leach, K. L.; Liu, S.; Marfat, A.; Marra, A.; McElroy, E.; Melnick, M.; Menard, C. A.; Montgomery, J. I.; Mullins, L.; Noe, M. C.; O'Donnell, J.; Penzien, J.; Plummer, M. S.; Price, L. M.; Shanmugasundaram, V.; Thoma, C.; Uccello, D. P.; Warmus, J. S.; Wishka, D. G. Potent Inhibitors of LpxC for the Treatment of Gram-Negative Infections. *J. Med. Chem.* **2011**, *55*, 914-923.

(11) McAllister, L. A.; Montgomery, J. I.; Abramite, J. A.; Reilly, U.; Brown, M. F.; Chen, J. M.; Barham, R. A.; Che, Y.; Chung, S. W.; Menard, C. A.; Mitton-Fry, M.; Mullins, L. M.; Noe, M. C.; O'Donnell, J. P.; Oliver, R. M.; Penzien, J. B.; Plummer, M.; Price, L. M.; Shanmugasundaram, V.; Tomaras, A. P.; Uccello, D. P. Heterocyclic methylsulfone hydroxamic acid LpxC inhibitors as Gram-negative antibacterial agents. *Bioorg. Med. Chem. Lett.* **2012**, *22*, 6832-6838.

(12) Jackman, J. E.; Fierke, C. A.; Tumey, L. N.; Pirrung, M.; Uchiyama, T.; Tahir, S. H.; Hindsgaul, O.; Raetz, C. R. H. Antibacterial agents that target lipid A biosynthesis in gram-negative bacteria: inhibition of diverse UDP-3-O-(R-3-hydroxymyristoyl)-N-acetylglucosamine deacetylases by substrate analogs containing zinc binding motifs. *J. Biol. Chem.* **2000**, *275*, 11002-11009.



- (13) Mdluli, K. E.; Witte, P. R.; Kline, T.; Barb, A. W.; Erwin, A. L.; Mansfield, B. E.; McClerren, A. L.; Pirrung, M. C.; Tumeay, L. N.; Warrenner, P.; Raetz, C. R. H.; Stover, C. K. Molecular validation of LpxC as an antibacterial drug target in *Pseudomonas aeruginosa*. *Antimicrob. Agents Chemother.* **2006**, *50*, 2178-2184.
- (14) Malkowski, S. N.; Grubb, C. S.; Peterson, L. W. "Synthesis of Natural Substrate Analogues to Probe the Active Site of LpxC in Gram-negative Bacteria" 2013;ORGN-257. American Chemical Society.
- (15) Clayton, G. M.; Klein, D. J.; Rickert, K. W.; Patel, S. B.; Kornienko, M.; Zugay-Murphy, J.; Reid, J. C.; Tummala, S.; Sharma, S.; Singh, S. B.; Miesel, L.; Lumb, K. J.; Soisson, S. M. Structure of the Bacterial Deacetylase LpxC Bound to the Nucleotide Reaction Product Reveals Mechanisms of Oxyanion Stabilization and Proton Transfer. *J. Biol. Chem.* **2013**, *288*, 34073-34080.
- (16) Dewar, A. J.; Johnson, S.; Malkowski, S. N.; Peterson, L.; Cafiero, M. "MP2 and DFT study of natural substrate analog interactions in the LpxC active site" 2014; CHED-622. American Chemical Society.
- (17) Buetow, L.; Dawson, A.; Hunter, W. N. The nucleotide-binding site of *Aquifex aeolicus* LpxC. *Acta Crystallographica Section F* **2006**, *62*, 1082-1086.
- (18) Malkowski, S. N.; Dewar, A. J.; Grubb, C. S.; Hatstat, A. K.; Cafiero, M.; Peterson, L. W. In *Tilte* 2014; American Chemical Society.
- (19) Bello, A. M.; Poduch, E.; Fujihashi, M.; Amani, M.; Li, Y.; Crandall, I.; Hui, R.; Lee, P. I.; Kain, K. C.; Pai, E. F.; Kotra, L. P. A Potent, Covalent Inhibitor of Orotidine 5'-Monophosphate Decarboxylase with Antimalarial Activity. *J. Med. Chem.* **2007**, *50*, 915-921.

- (20) Winans, K. A.; Bertozzi, C. R. An Inhibitor of the Human UDP-GlcNAc 4-Epimerase Identified from a Uridine-Based Library. A Strategy to Inhibit O-Linked Glycosylation. *Chem. Biol.* **2002**, *9*, 113-129.
- (21) Wang, R.; Steensma, D. H.; Takaoka, Y.; Yun, J. W.; Kajimoto, T.; Wong, C.-H. A search for pyrophosphate mimics for the development of substrates and inhibitors of glycosyltransferases. *Bioorg. Med. Chem.* **1997**, *5*, 661-672.
- (22) Wagner, H.; Brinks, M. K.; Hirtz, M.; Schaefer, A.; Chi, L.-F.; Studer, A. Chemical Surface Modification of Self-Assembled Monolayers by Radical Nitroxide Exchange Reactions. *Chem.--Eur. J.* **2011**, *17*, 9107-9112, S9107/9101-S9107/9189.
- (23) Jawalekar, A. M.; Meeuwenoord, N.; Cremers, J. G. O.; Overkleeft, H. S.; van der Marel, G. A.; Rutjes, F. P. J. T.; van Delft, F. L. Conjugation of Nucleosides and Oligonucleotides by [3+2] Cycloaddition. *J. Org. Chem.* **2008**, *73*, 287-290.
- (24) Sauer, R.; El-Tayeb, A.; Kaulich, M.; Mueller, C. E. Synthesis of uracil nucleotide analogs with a modified, acyclic ribose moiety as P2Y2 receptor antagonists. *Bioorg. Med. Chem.* **2009**, *17*, 5071-5079.
- (25) Semaine, W.; Johar, M.; Tyrrell, D. L. J.; Kumar, R.; Agrawal, B. Inhibition of Hepatitis B Virus (HBV) Replication by Pyrimidines Bearing an Acyclic Moiety: Effect on Wild-Type and Mutant HBV. *J. Med. Chem.* **2006**, *49*, 2049-2054.
- (26) Ubasawa, M.; Takashima, H.; Sekiya, K. A convenient one-pot synthesis of acyclic nucleosides. *Chem. Pharm. Bull.* **1995**, *43*, 142-143.
- (27) Srivastav, N. C.; Manning, T.; Kunimoto, D. Y.; Kumar, R. Studies on acyclic pyrimidines as inhibitors of mycobacteria. *Bioorg. Med. Chem.* **2007**, *15*, 2045-2053.

(28) Zhang, X.; Shen, X.; Yan, H.; Chen, H. Synthesis, spectroscopic characterization, axial base coordination equilibrium and photolytic kinetics studies of a new coenzyme B12 analogue-3[prime or minute]-deoxy-2[prime or minute],3[prime or minute]-anhydrothymidylcobalamin. *Dalton Transactions* **2007**, 2336-2342.

(29) Lin, T. S.; Prusoff, W. H. A novel synthesis and biological activity of several 5-halo-5'-amino analogues of deoxyribopyrimidine nucleosides. *J. Med. Chem.* **1978**, *21*, 106-109.

(30) Kawaguchi, M.; Okabe, T.; Okudaira, S.; Nishimasu, H.; Ishitani, R.; Kojima, H.; Nureki, O.; Aoki, J.; Nagano, T. Screening and X-ray Crystal Structure-based Optimization of Autotaxin (ENPP2) Inhibitors, Using a Newly Developed Fluorescence Probe. *ACS Chem. Biol.* **2013**, *8*, 1713-1721.

(31) Suzuki, T.; Ota, Y.; Ri, M.; Bando, M.; Gotoh, A.; Itoh, Y.; Tsumoto, H.; Tatum, P. R.; Mizukami, T.; Nakagawa, H.; Iida, S.; Ueda, R.; Shirahige, K.; Miyata, N. Rapid Discovery of Highly Potent and Selective Inhibitors of Histone Deacetylase 8 Using Click Chemistry to Generate Candidate Libraries. *J. Med. Chem.* **2012**, *55*, 9562-9575.

(32) Giacomelli, G.; Porcheddu, A.; Salaris, M. Simple One-Flask Method for the Preparation of Hydroxamic Acids. *Org. Lett.* **2003**, *5*, 2715-2717.

## VI. Appendix

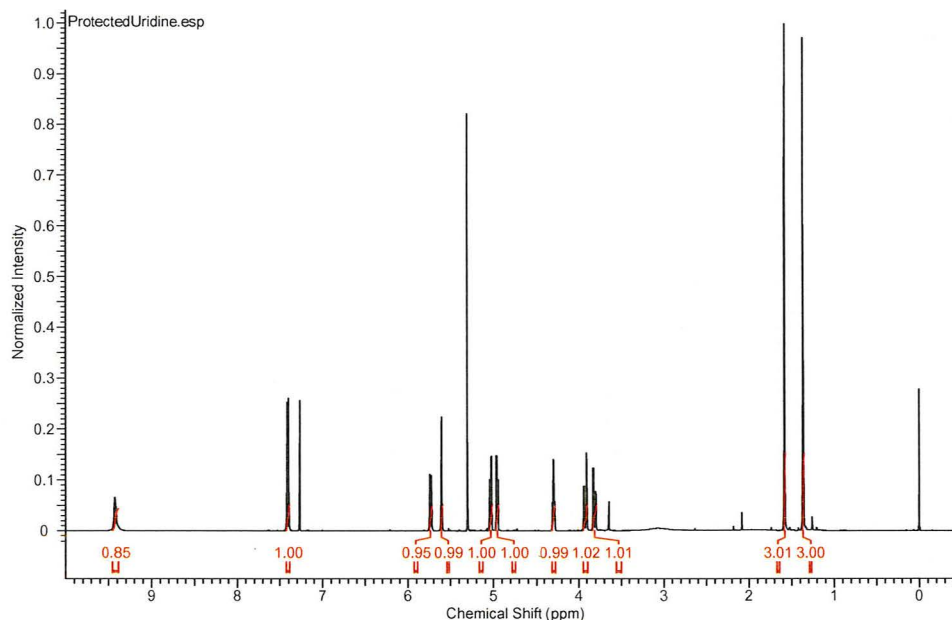


**Figure A1.**  $^1\text{H}$  NMR of 1-((3aR,4R,6R,6aR)-6-(hydroxymethyl)-2,2-dimethyltetrahydrofuro[3,4-d][1,3]dioxol-4-yl)pyrimidine-2,4(1H,3H)-dione (**1**).  $^1\text{H}$  NMR ( $\text{CHCl}_3-d$ ):  $\delta$  1.36 (s, 3 H) 1.58 (s, 3 H) 3.81 (dd,  $J = 12.1, 3.67$  Hz, 1 H) 3.92 (dd,  $J = 12.1, 2.69$  Hz, 1 H) 4.29 (q,  $J = 3.4$  Hz, 1 H) 4.96 (dd,  $J = 6.4, 3.45$  Hz, 1 H) 5.04 (dd,  $J = 6.5, 2.93$  Hz, 1 H) 5.61 (d,  $J = 2.9$  Hz, 1 H) 5.74 (d,  $J = 8.4$  Hz, 1 H) 7.41 (d,  $J = 8.0$  Hz, 1 H) 9.42 (br. s., 1 H)

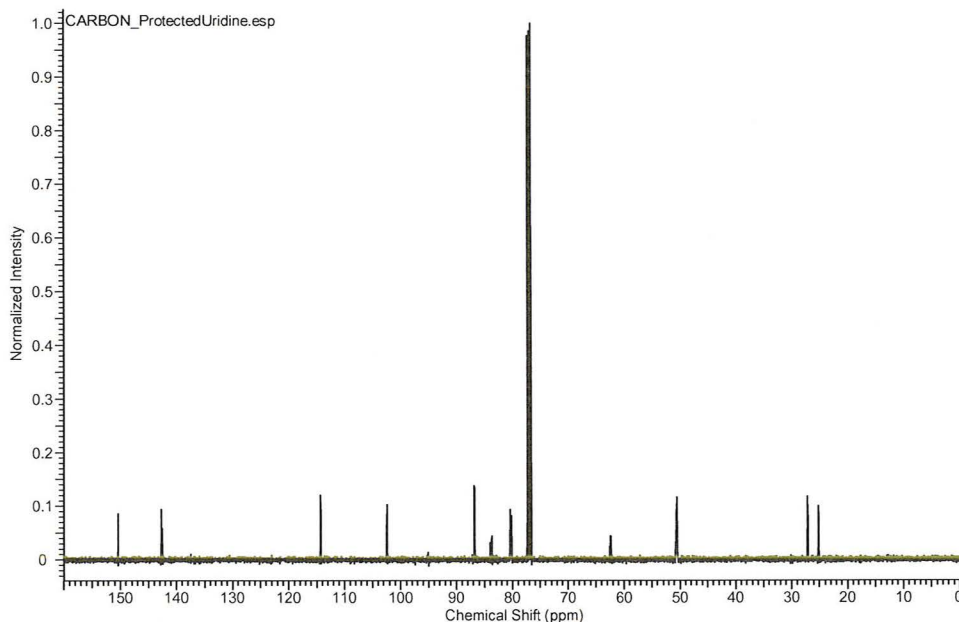


**Figure A2.**  $^{13}\text{C}$  NMR of 1-((3aR,4R,6R,6aR)-6-(hydroxymethyl)-2,2-dimethyltetrahydrofuro[3,4-d][1,3]dioxol-4-yl)pyrimidine-2,4(1H,3H)-dione (**1**).  $^{13}\text{C}$  NMR ( $\text{CHCl}_3-d$ ):  $\delta$  25.19, 27.15, 50.56, 62.38, 80.17, 80.42, 83.69, 86.83, 102.40, 114.30, 142.72, 150.44

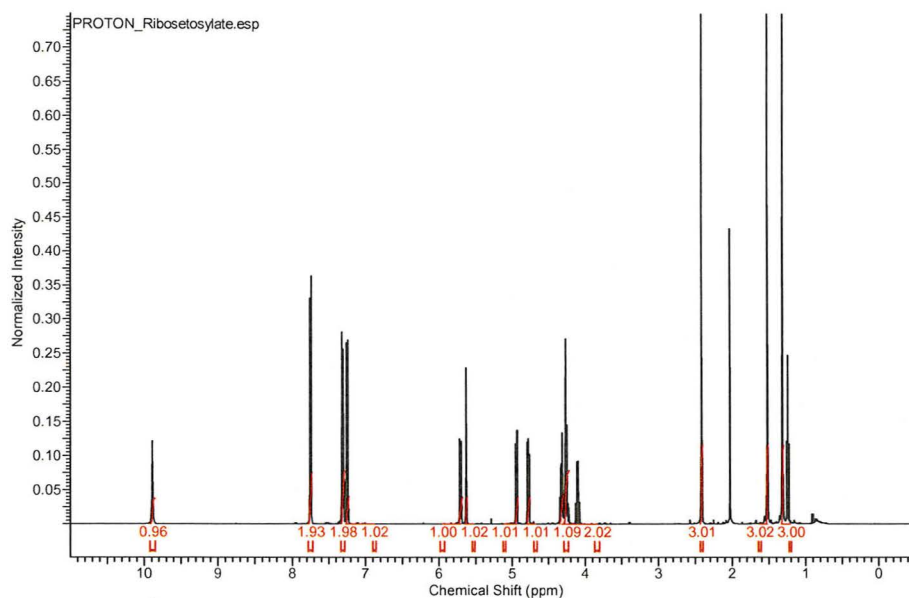


**Figure A3.**  $^1\text{H}$  NMR of ((3aR,4R,6R,6aR)-6-(2,4-dioxo-3,4-dihydropyrimidin-1(2H)-yl)-2,2-dimethyltetrahydrofuro[3,4-d][1,3]dioxol-4-yl)methyl 4-methylbenzenesulfonate (**2**).  $^1\text{H}$  NMR ( $\text{CHCl}_3-d$ ):  $\delta$  1.31 (s, 3 H) 1.52 (s, 3 H) 2.41 (s, 3 H) 4.22 - 4.29 (m, 2 H) 4.29 - 4.35 (m, 1 H) 4.78 (dd,  $J = 6.38$ , 3.74 Hz, 1 H) 4.94 (dd,  $J = 6.4$ , 1.98 Hz, 1 H) 5.63 (d,  $J = 2.0$  Hz, 1 H) 5.71 (d,  $J = 8.1$  Hz, 1 H) 7.24 (d,  $J = 8.1$  Hz, 1 H) 7.31 (d,  $J = 8.0$  Hz, 2 H) 7.74 (d,  $J = 8.3$  Hz, 2 H) 9.89 (s, 1 H)

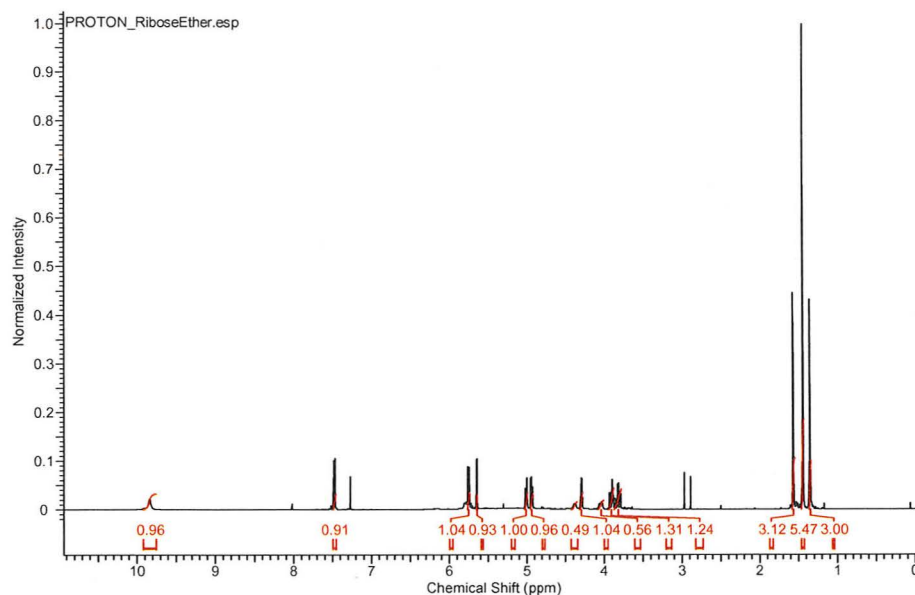


**Figure A4.**  $^1\text{H}$  NMR of N-(*tert*-butoxycarbonyl)-O-(((3aR,4R,6R,6aR)-6-(2,4-dioxo-3,4-dihydropyrimidin-1(2H)-yl)-2,2-dimethyltetrahydrofuro[3,4-d][1,3]dioxol-4-yl)methyl)-L-serine (**3**).  $^1\text{H}$  NMR ( $\text{CHCl}_3-d$ ):  $\delta$  1.36 (s, 3 H) 1.45 (s, 5 H) 1.57 (s, 3 H) 3.77 - 3.87 (m, 1 H) 3.87 - 3.94 (m, 1 H) 4.00 - 4.07 (m, 1 H) 4.29 (q,  $J = 3.2$  Hz, 1 H) 4.38 (br. s., 1 H) 4.94 (dd,  $J = 6.4$ , 3.45 Hz, 1 H) 5.01 (dd,  $J = 6.4$ , 2.84 Hz, 1 H) 5.64 (d,  $J = 2.8$  Hz, 1 H) 5.75 (d,  $J = 8.0$  Hz, 1 H) 7.47 (d,  $J = 8.0$  Hz, 1 H) 9.84 (br. s., 1 H)

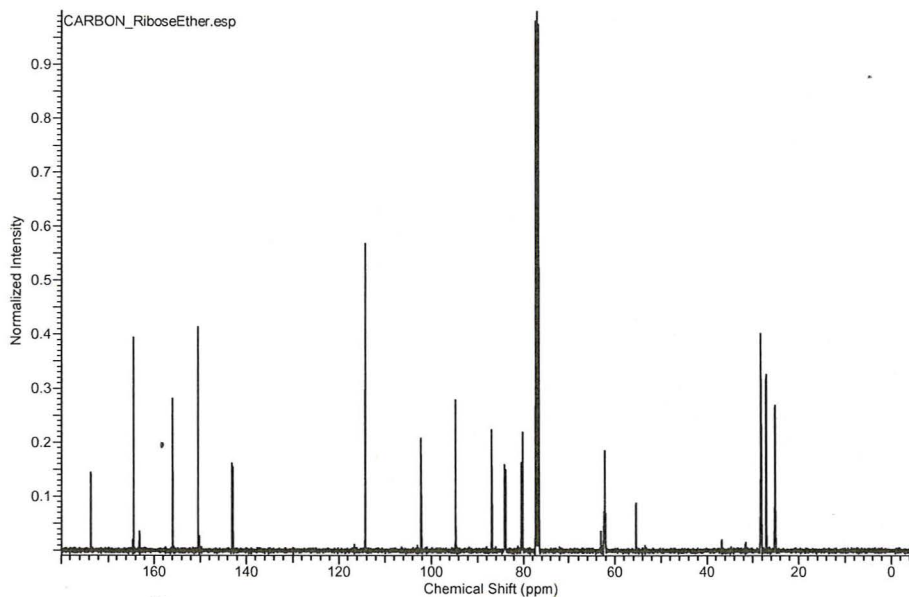


**Figure A5.**  $^{13}\text{C}$  NMR of N-(tert-butoxycarbonyl)-O-(((3aR,4R,6R,6aR)-6-(2,4-dioxo-3,4-dihydropyrimidin-1(2H)-yl)-2,2-dimethyltetrahydrofuro[3,4-d][1,3]dioxol-4-yl)methyl)-L-serine (**3**).  $^{13}\text{C}$  NMR ( $\text{CHCl}_3-d$ ):  $\delta$  25.11, 27.10, 28.21, 55.45, 62.20, 80.18, 83.84, 86.86, 94.68, 102.21, 114.23, 143.09, 150.46, 155.96, 164.38, 173.68

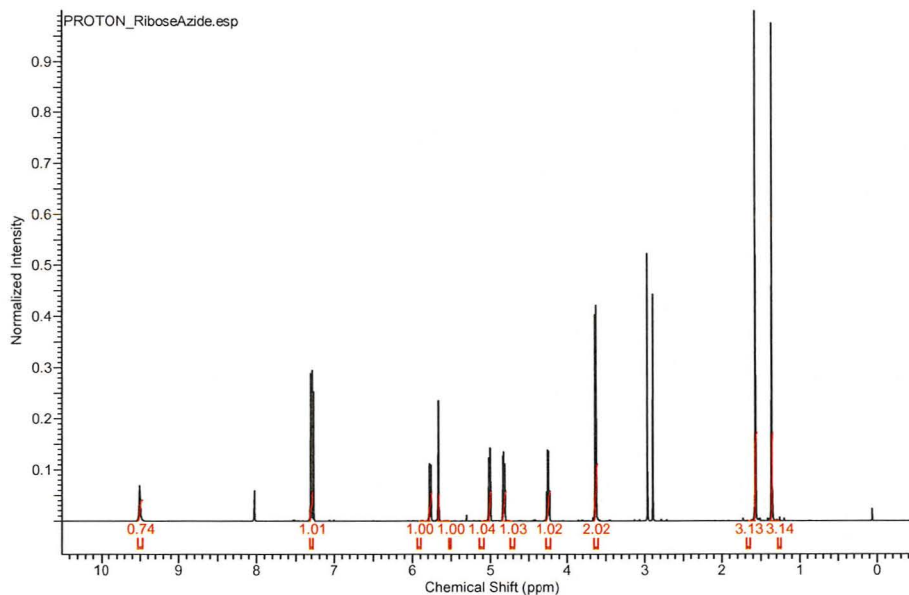


**Figure A6.**  $^1\text{H}$  NMR of 1-((3aR,4R,6R,6aR)-6-(azidomethyl)-2,2-dimethyltetrahydrofuro[3,4-d][1,3]dioxol-4-yl)pyrimidine-2,4(1H,3H)-dione (**5**).  $^1\text{H}$  NMR ( $\text{CHCl}_3-d$ ):  $\delta$  1.36 (s, 3 H) 1.57 (s, 3 H) 3.63 (d,  $J = 5.3$  Hz, 2 H) 4.24 (q,  $J = 5.0$  Hz, 1 H) 4.82 (dd,  $J = 6.5, 4.18$  Hz, 1 H) 5.01 (dd,  $J = 6.5, 2.15$  Hz, 1 H) 5.66 (d,  $J = 2.2$  Hz, 1 H) 5.77 (d,  $J = 8.0$  Hz, 1 H) 7.30 (d,  $J = 8.1$  Hz, 1 H) 9.50 (br. s., 1 H)

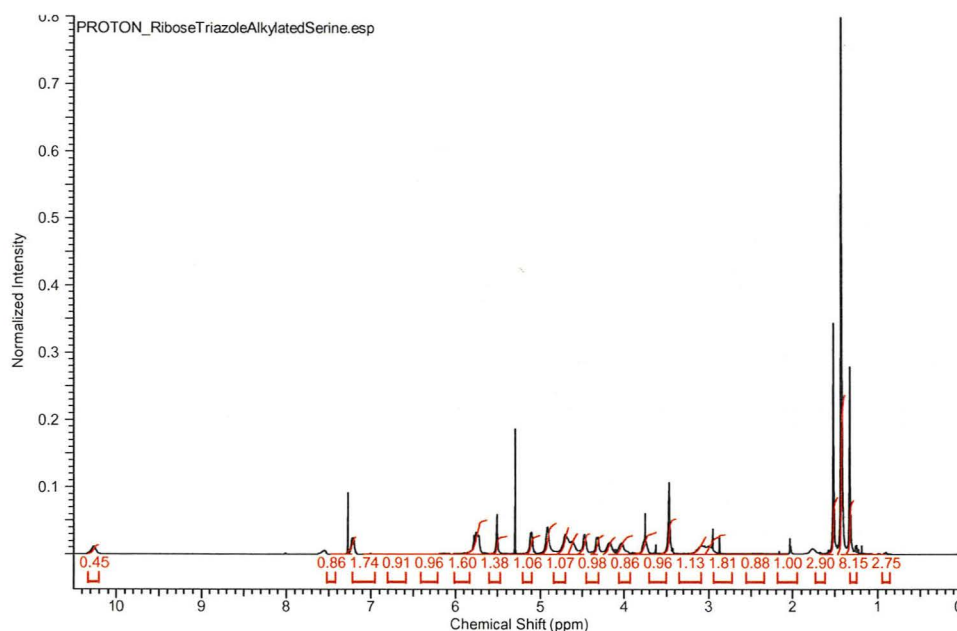


**Figure A7.**  $^1\text{H}$  NMR of *N*-(*tert*-butoxycarbonyl)-*O*-(2-(1-(((3*aR*,4*R*,6*R*,6*aR*)-6-(2,4-dioxo-3,4-dihydropyrimidin-1(2*H*)-yl)-2,2-dimethyltetrahydrofuro[3,4-*d*][1,3]dioxol-4-yl)methyl)-1*H*-1,2,3-triazol-4-yl)ethyl)-*L*-serine (**6**).  $^1\text{H}$  NMR ( $\text{CHCl}_3$ -*d*):  $\delta$  1.33 (s, 3 H) 1.42 (s, 8 H) 1.52 (s, 3 H) 2.99 (br. s., 1 H) 3.09 (br. s., 1 H) 3.47 (br. s., 2 H) 3.76 (s, 1 H) 4.03 (br. s., 1 H) 4.18 (br. s., 1 H) 4.32 (d,  $J=7.2$  Hz, 1 H) 4.47 (br. s., 1 H) 4.63 (br. s., 1 H) 4.70 (br. s., 1 H) 4.92 (br. s., 2 H) 5.01 - 5.21 (m, 1 H) 5.51 (br. s., 1 H) 5.75 (dd,  $J = 14.1, 7.85$  Hz, 2 H) 7.21 (d,  $J = 7.1$  Hz, 1 H) 10.27 (br. s., 1 H)

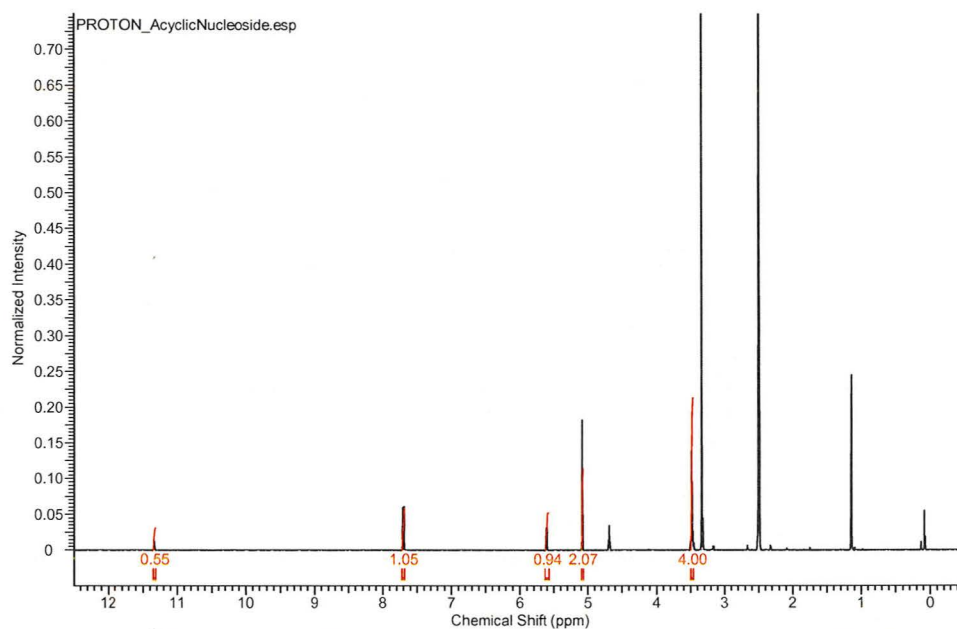


**Figure A8.**  $^1\text{H}$  NMR of 1-((2-hydroxyethoxy)methyl)pyrimidine-2,4(1*H*,3*H*)-dione (**7**).  $^1\text{H}$  NMR ( $\text{DMSO-}d_6$ ):  $\delta$  3.46 - 3.50 (m, 4 H) 5.08 (s, 2 H) 5.61 (d,  $J = 7.9$  Hz, 1 H) 7.70 (d,  $J = 7.9$  Hz, 1 H) 11.34 (s, 1 H)

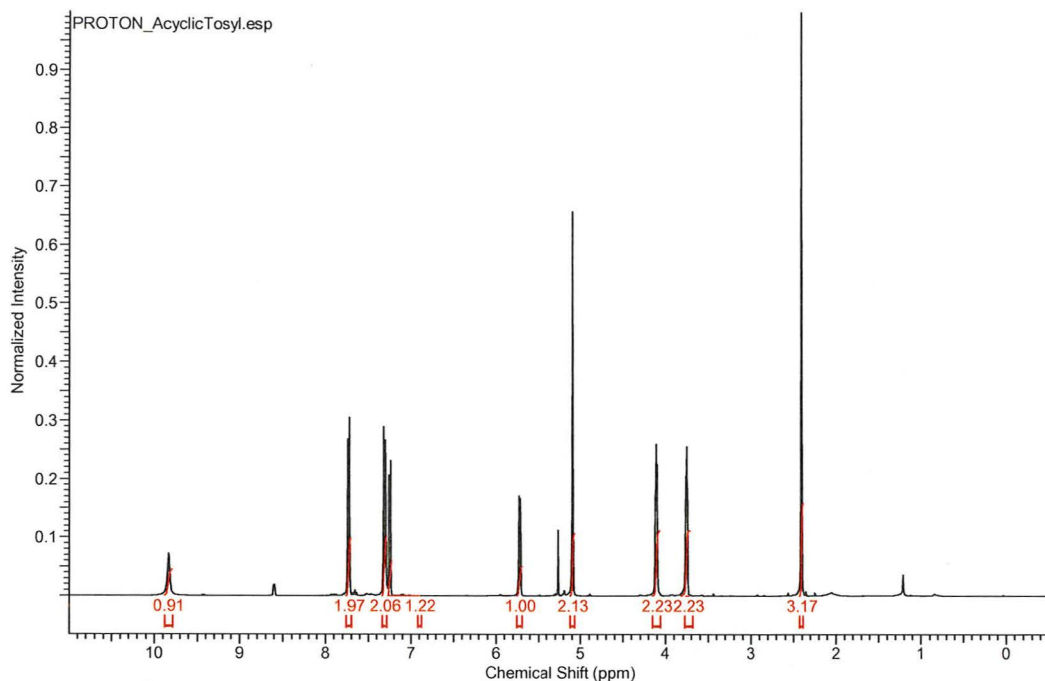


**Figure A9.**  $^1\text{H}$  NMR of 2-((2,4-dioxo-3,4-dihydropyrimidin-1(2H)-yl)methoxy)ethyl 4-methylbenzenesulfonate (**8**).  $^1\text{H}$  NMR ( $\text{CHCl}_3$ -*d*):  $\delta$  2.41 (s, 3 H) 3.76 (t,  $J = 4.4$  Hz, 2 H) 4.11 (t,  $J = 4.5$  Hz, 2 H) 5.10 (s, 2 H) 5.72 (d,  $J = 6.9$  Hz, 1 H) 7.25 (d,  $J = 7.9$  Hz, 1 H) 7.31 (d,  $J = 7.8$  Hz, 2 H) 7.73 (d,  $J = 7.1$  Hz, 2 H) 9.84 (br. s., 1 H)

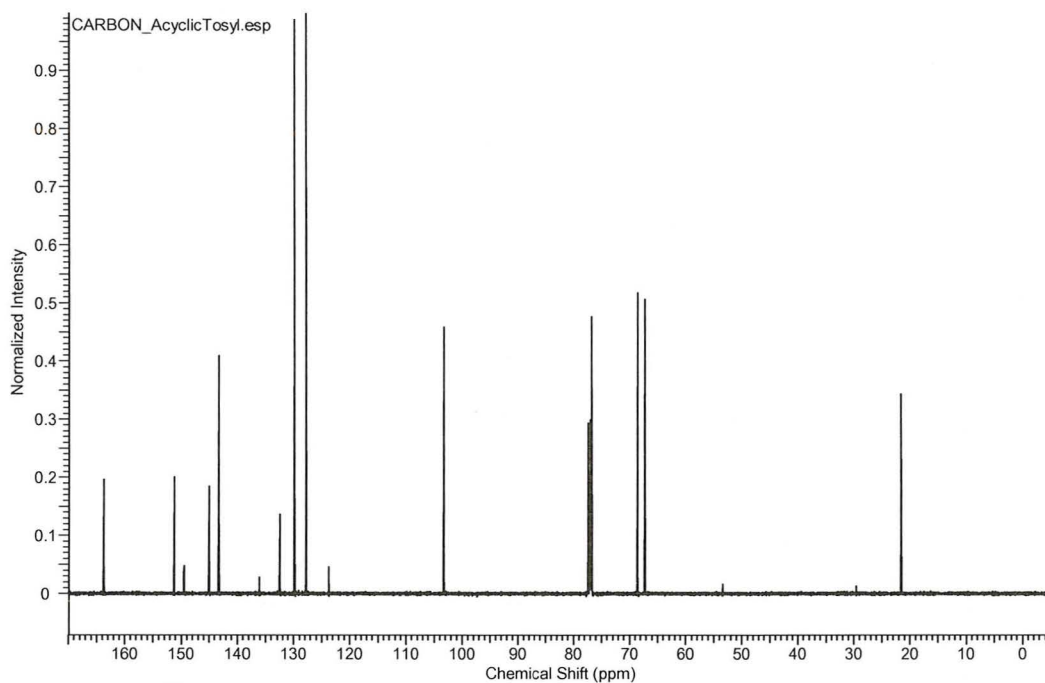


**Figure A10.**  $^{13}\text{C}$  NMR of 2-((2,4-dioxo-3,4-dihydropyrimidin-1(2H)-yl)methoxy)ethyl 4-methylbenzenesulfonate (**8**).  $^{13}\text{C}$  NMR ( $\text{CHCl}_3$ -*d*):  $\delta$  21.58, 67.24, 68.55, 103.29, 127.81, 129.85, 132.52, 143.26, 145.04, 151.24, 163.69



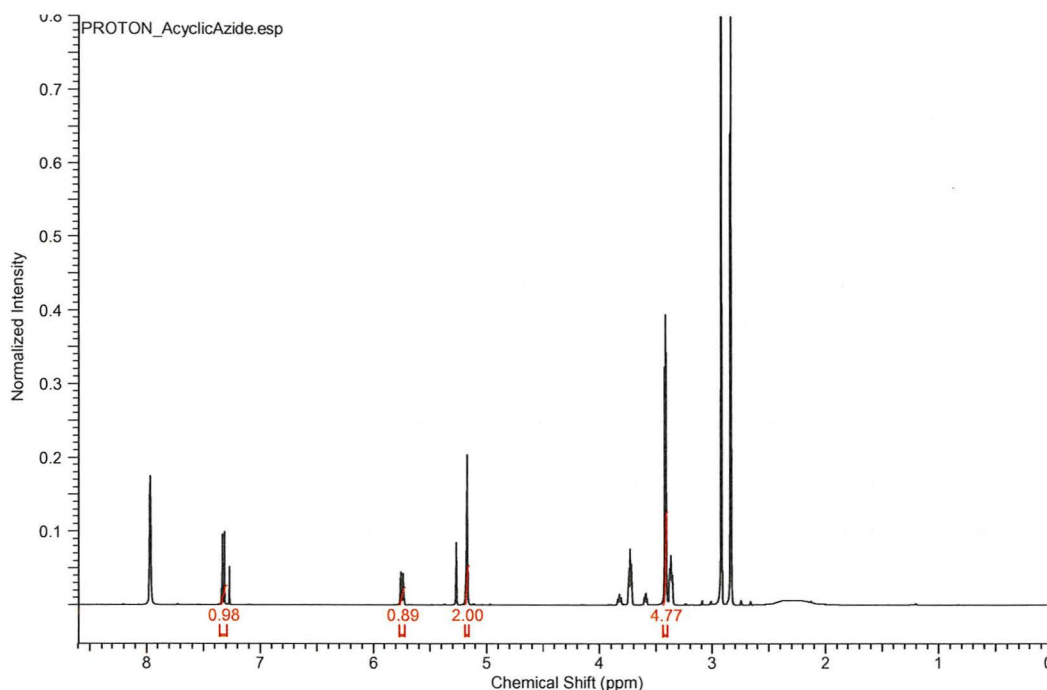


**Figure A11.**  $^1\text{H}$  NMR of 1-((2-azidoethoxy)methyl)pyrimidine-2,4(1H,3H)-dione (**9**).  $^1\text{H}$  NMR ( $\text{CHCl}_3-d$ ):  $\delta$  3.40 - 3.44 (m, 5 H) 5.18 (d,  $J = 1.7$  Hz, 2 H) 5.75 (dt,  $J = 7.9, 1.59$  Hz, 1 H) 7.32 (d,  $J = 7.9$  Hz, 1 H)

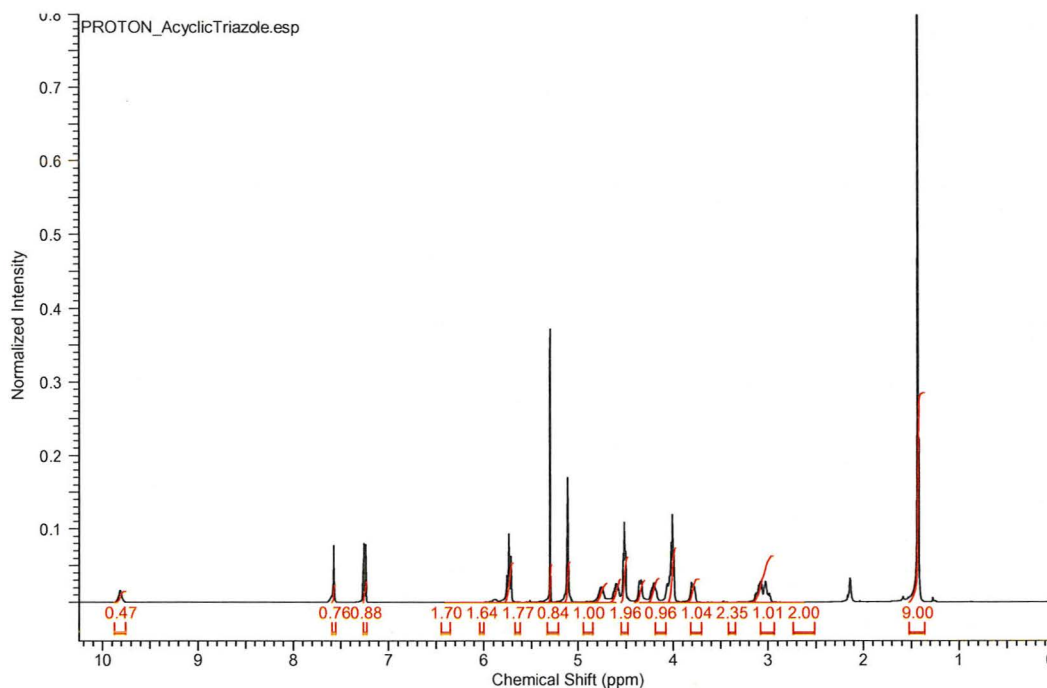


**Figure A12.**  $^1\text{H}$  NMR of *N*-(*tert*-butoxycarbonyl)-*O*-(2-(1-(2-((2,4-dioxo-3,4-dihydropyrimidin-1(2H)-yl)methoxy)ethyl)-1H-1,2,3-triazol-4-yl)ethyl)-*L*-serine (**10**).  $^1\text{H}$  NMR ( $\text{CHCl}_3-d$ ):  $\delta$  1.43 (s, 9 H) 2.95 - 3.17 (m, 2 H) 3.79 (d,  $J = 10.76$  Hz, 1 H) 4.01 (t,  $J = 4.79$  Hz, 2 H) 4.15 - 4.27 (m, 1 H) 4.35 (d,  $J = 8.12$  Hz, 1 H) 4.52 (t,  $J = 4.84$  Hz, 2 H) 4.56 - 4.66 (m, 1 H) 4.76 (br. s., 1 H) 5.11 (s, 2 H) 5.30 (d,  $J = 1.37$  Hz, 2 H) 5.69 - 5.78 (m, 2 H) 7.25 (dd,  $J = 7.92, 1.17$  Hz, 1 H) 7.57 (s, 1 H) 9.81 (br. s., 1 H)

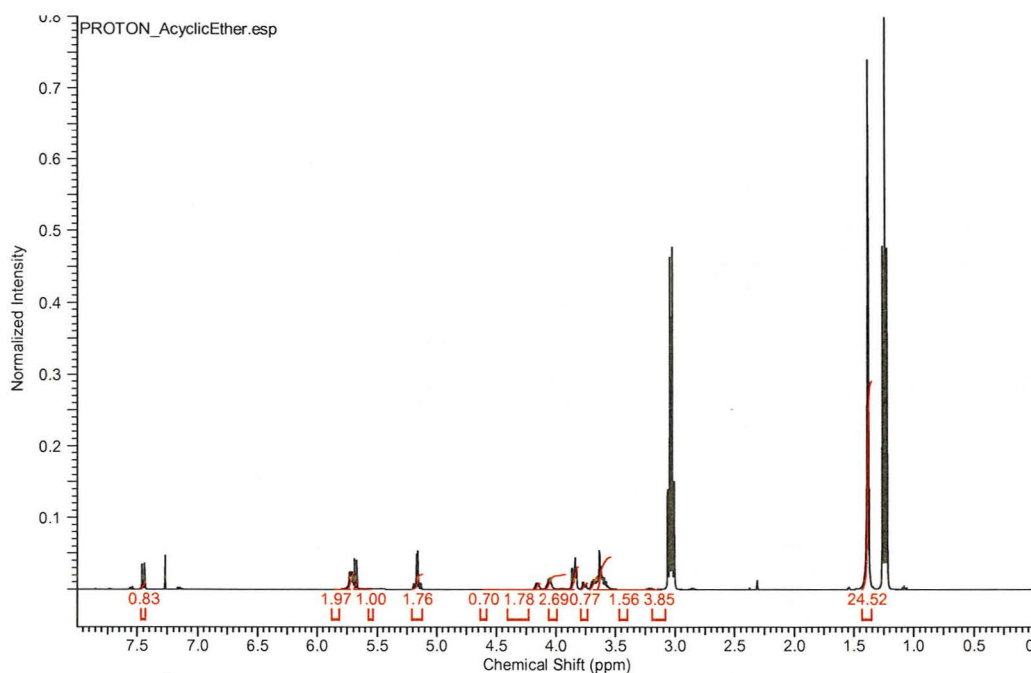


**Figure A13.**  $^1\text{H}$  NMR of *N*-(*tert*-butoxycarbonyl)-*O*-(2-((2,4-dioxo-3,4-dihydropyrimidin-1(2H)-yl)methoxy)ethyl)-*L*-serine (**11**).  $^1\text{H}$  NMR ( $\text{CHCl}_3$ -*d*):  $\delta$  1.38 (s, 25 H) 3.54 - 3.65 (m, 4 H) 3.65 - 3.72 (m, 2 H) 3.73 - 3.79 (m, 1 H) 3.85 (dd,  $J$  = 10.2, 4.77 Hz, 3 H) 4.06 (q,  $J$  = 5.4 Hz, 2 H) 4.16 (dt,  $J$  = 7.0, 3.33 Hz, 1 H) 5.16 (q,  $J$  = 10.3 Hz, 2 H) 5.68 (d,  $J$  = 8.2 Hz, 1 H) 5.73 (d,  $J$  = 6.6 Hz, 2 H) 7.45 (d,  $J$  = 7.9 Hz, 1 H)

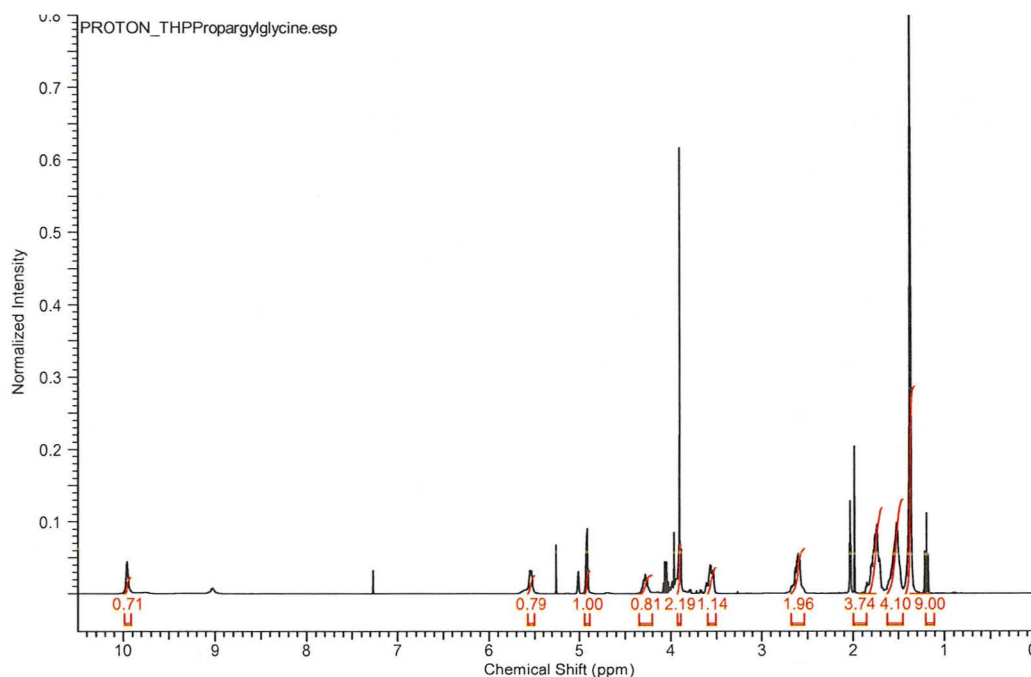


**Figure A14.**  $^1\text{H}$  NMR of *tert*-butyl ((2*S*)-1-oxo-1-(((tetrahydro-2H-pyran-2-yl)oxy)amino)-pent-4-yn-2-yl)carbamate (**12**).  $^1\text{H}$  NMR ( $\text{CHCl}_3$ -*d*):  $\delta$  1.38 (s, 9 H) 1.46 - 1.63 (m, 4 H) 1.68 - 1.83 (m, 4 H) 2.60 (br. s., 2 H) 3.55 (d,  $J$  = 11.0 Hz, 1 H) 3.91 (s, 2 H) 4.28 (t,  $J$  = 7.0 Hz, 1 H) 4.92 (d,  $J$  = 2.5 Hz, 1 H) 5.54 (d,  $J$  = 7.7 Hz, 1 H) 9.96 (br. s., 1 H)

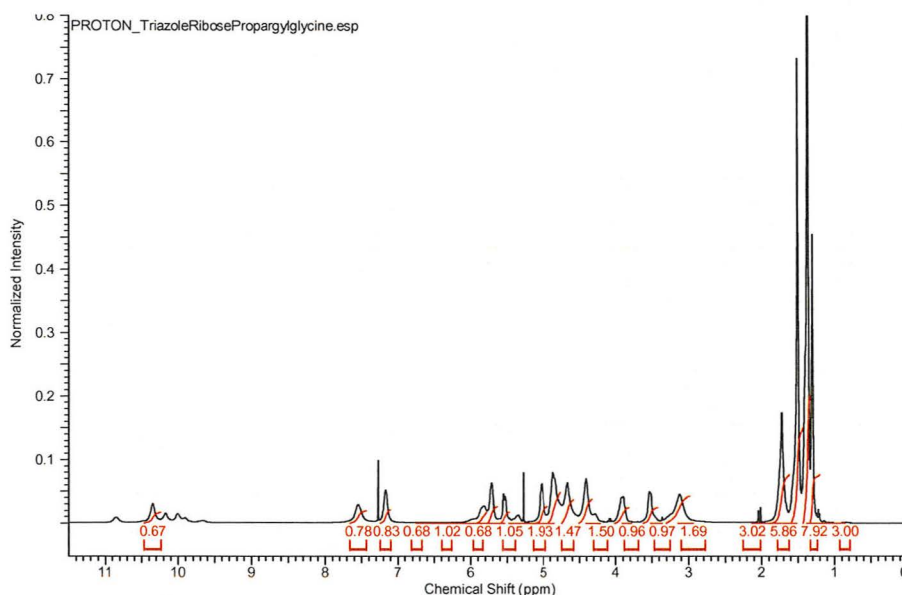


**Figure A15.**  $^1\text{H}$  NMR of tert-butyl ((2S)-3-(1-(((3aR,4R,6R,6aR)-6-(2,4-dioxo-3,4-dihydropyrimidin-1(2H)-yl)-2,2-dimethyltetrahydrofuro[3,4-d][1,3]dioxol-4-yl)methyl)-1H-1,2,3-triazol-4-yl)-1-oxo-1-((tetrahydro-2H-pyran-2-yl)oxy)amino)propan-2-yl)carbamate (**13**).  $^1\text{H}$  NMR ( $\text{CHCl}_3-d$ ):  $\delta$  1.30 (br. s., 3 H) 1.37 (br. s., 8 H) 1.50 (br. s., 6 H) 1.72 (br. s., 3 H) 3.12 (br. s., 1 H) 3.54 (br. s., 1 H) 3.91 (d,  $J = 8.8$  Hz, 1 H) 4.41 (br. s., 1 H) 4.67 (br. s., 1 H) 4.86 (br. s., 1 H) 5.02 (br. s., 1 H) 5.54 (d,  $J = 10.2$  Hz, 1 H) 5.71 (br. s., 1 H) 5.82 (br. s., 1 H) 7.16 (br. s., 1 H) 7.43 - 7.66 (m, 1 H) 10.24 - 10.47 (m, 1 H)

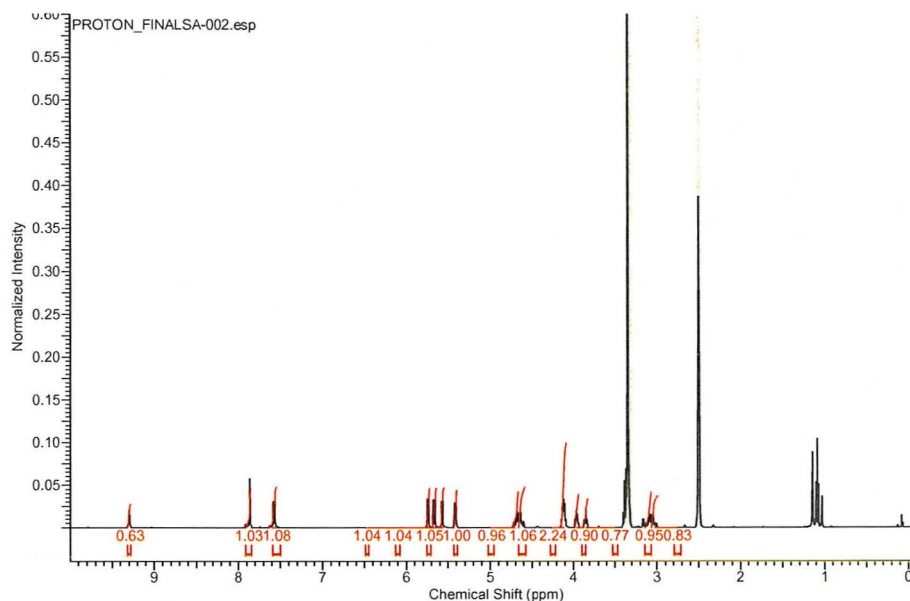


**Figure A16.**  $^1\text{H}$  NMR of (S)-2-amino-3-(1-(((2R,3S,4R,5R)-5-(2,4-dioxo-3,4-dihydropyrimidin-1(2H)-yl)-3,4-dihydroxytetrahydrofuran-2-yl)methyl)-1H-1,2,3-triazol-4-yl)-N-hydroxypropanamide (**14**).  $^1\text{H}$  NMR ( $\text{DMSO}-d_6$ ):  $\delta$  ppm 3.04 (dd,  $J = 15.0$ , 7.19 Hz, 1 H) 3.11 (dd,  $J = 15.0$ , 6.75 Hz, 1 H) 3.85 (t,  $J = 7.0$  Hz, 1 H) 3.96 (q,  $J = 5.2$  Hz, 1 H) 4.12 (quin,  $J = 5.1$  Hz, 2 H) 4.63 (dd,  $J = 14.5$ , 7.68 Hz, 1 H) 4.70 (dd,  $J = 14.5$ , 4.06 Hz, 1 H) 5.41 (d,  $J = 5.5$  Hz, 1 H) 5.57 (d,  $J = 5.5$  Hz, 1 H) 5.66 (d,  $J = 8.0$  Hz, 1 H) 5.74 (d,  $J = 5.2$  Hz, 1 H) 7.57 (d,  $J = 8.1$  Hz, 1 H) 7.86 (s, 1 H) 9.30 (s, 1 H)